SECURITY CLASSIFICATION OF THIS PAGE

REPORT DOCUMENTATION PAGE

1a. REPORT SECURITY CLASSIFICATION None	1b. RESTRICTIVE MARKINGS None
2a. SECURITY CLASSIFICATION AUTHORITY None	3. DISTRIBUTION / AVAILABILITY OF REPORT This document has been approved for public release and sale; its distribution is unlimited.
2b. DECLASSIFICATION / DOWNGRADING SCHEDULE None	
4. PERFORMING ORGANIZATION REPORT NUMBER(S)	5. MONITORING ORGANIZATION REPORT NUMBER(S)
6a. NAME OF PERFORMING ORGANIZATION University of Cincinnati 6b. OFFICE SYMBOL (*If applicable*)	7a. NAME OF MONITORING ORGANIZATION Office of Naval Research
6c. ADDRESS (*City, State, and ZIP Code*) Department of MAterials Science & Engineering Cincinnati, OH 45221-0012	7b. ADDRESS (*City, State, and ZIP Code*) 800 North Quincy Street Arlington, VA 22217
8a. NAME OF FUNDING / SPONSORING ORGANIZATION Office of Naval Research 8b. OFFICE SYMBOL (*If applicable*)	9. PROCUREMENT INSTRUMENT IDENTIFICATION NUMBER N00014-93-1-0144
8c. ADDRESS (*City, State, and ZIP Code*) 800 North Quincy Street Arlington, VA 22217	10. SOURCE OF FUNDING NUMBERS PROGRAM ELEMENT NO. / PROJECT NO. / TASK NO. adh 9302 / WORK UNIT ACCESSION NO.

11. TITLE (*Include Security Classification*)
Effect of Processing Variables on the Structure and Properties of Polymer Interphases

12. PERSONAL AUTHOR(S)
F. J. Boerio

13a. TYPE OF REPORT	13b. TIME COVERED	14. DATE OF REPORT (*Year, Month, Day*)	15. PAGE COUNT
Final	FROM 12/1/92 TO 11/30/96	July 15, 1998	50

16. SUPPLEMENTARY NOTATION

17. COSATI CODES			18. SUBJECT TERMS (*Continue on reverse if necessary and identify by block number*)
FIELD	GROUP	SUB-GROUP	

19. ABSTRACT (*Continue on reverse if necessary and identify by block number*)

The effect of processing variables on the molecular structure and properties of interphases formed between polyimides and metal substrates was determined. Polyimide films were formed on aluminum substrates by spin-coating of polyamic acid followed by thermal imidization and by vapor-codeposition of the monomers followed by thermal imidization. Spin-coating of polyamic acid and thermal imidization were also used to deposit polyimide films on gold substrates. Films were formed on silver substrates by Langmuir-Blodgett deposition of alkylamine salts of polyamic acid followed by chemical imidization. 4-mercaptophenylphthalimide, a model polyimide, was adsorbed onto gold substrates by adsorption from solution. The films were characterized as appropriate by X-ray photoelectron spectroscopy (XPS), reflection-absorption infrared spectroscopy (RAIR), and surface-enhanced Raman scattering (SERS). The fracture energy required to delaminate polyimide films from aluminum and gold substrates was determined using the circular blister test. Finite element analysis was used to determine the effects of plastic deformation on a global scale on the fracture energy.

20. DISTRIBUTION / AVAILABILITY OF ABSTRACT ☒ UNCLASSIFIED/UNLIMITED ☐ SAME AS RPT. ☐ DTIC USERS	21. ABSTRACT SECURITY CLASSIFICATION Unclassified
22a. NAME OF RESPONSIBLE INDIVIDUAL Dr. Peter P. Schmidt	22b. TELEPHONE (*Include Area Code*) (703) 696-4362 22c. OFFICE SYMBOL

DD FORM 1473, 84 MAR 83 APR edition may be used until exhausted. All other editions are obsolete.

SECURITY CLASSIFICATION OF THIS PAGE

19. Abstract (continued)

Assuming an elastic analysis, the fracture energy required to delaminate a spin-coated film from an aluminum substrate was about 647 J/m^2. The fracture energy required to delaminate a vapor-deposited film was 995 J/m^2 while the fracture energy required to delaminate a spin-coated film from an aluminum substrate that had been pre-treated with a thin film of γ-aminopropyltriethoxysilane was about 1298 J/m^2. The fracture energy required to delaminate spin-coated PMDA/ODA films from gold was relatively low, about 422 J/m^2. These values were all much greater than the surface energy of typical polyimides, indicating that energy dissipation due to plastic deformation made an important contribution to the fracture energy. However, plastic deformation on a global scale made up only about 15% of the fracture energy, indicating that other processes, such as plasticity at the crack tip, were very important.

Formation of carboxylate salts in the aluminum/film interphase led to the partial imidization of polyimide films in the interphase. This interphase acted as a weak boundary layer, and was the locus of failure during fracture mechanics experiments. Carboxylate salt formation was highest for spin-coated films on aluminum, lowest for spin-coated films on silanated aluminum substrates, and intermediate for vapor-deposited films. The fracture energy of polyimide films on aluminum substrates was thus closely correlated with carboxylate formation in the interphase.

Langmuir-Blodgett (LB) films of alkylamine salts of the polyamic acid of PMDA/ODA were deposited onto silver substrates mainly as salts which were easily imidized. After imidization, the axis of the PMDA moieties was tilted away from the surface normal by about 70°, showing that the molecular axis of the PMDA/PDA polyimide molecules had a preferred orientation which was nearly parallel to the silver surface.

4-mercaptophenylphthalimide (4-MPP) was chemisorbed onto gold surfaces through the thiol groups to form an oriented monolayer. The molecules were oriented with a vertical configuration in which the molecular axes tilted away from the surface normal by about 21°. There was no preferred orientation with respect to rotation about the molecular axes. These results were in excellent agreement with those obtained from molecular dynamics simulations.

I. Introduction

Polyimides have a combination of properties that have contributed to their widespread use in the microelectronics industry. Included are good thermal and mechanical stability, excellent dielectric properties, chemical resistance, and good film forming characteristics [1-3]. Successful adhesion of polyimides to metals is crucial in microelectronics applications. It is well known that the adhesion is largely dependent on the physical and chemical interactions that occur at the polymer/metal interface. Therefore, understanding the interface chemistry and its effect on polyimide/metal adhesion is vitally important in microelectronic applications of polyimides.

Most polyimides used in microelectronics are prepared by reaction of pyromellitic dianhydride (PMDA) and oxydianiline (ODA) to form a polyamic acid (PAA). Films are usually applied to substrates by spin coating a solution of PAA in a strong solvent such as n-methylpyrollidone (NMP). The films are then heated to drive off the solvent and to convert the PAA to the corresponding polyimide. Alternatively, the PAA films can be chemically imidized. However, handling of PAA solutions raises several important issues. The solvents strongly complex with the PAA and require heating to temperatures above 90°C for complete removal [4-6]. Decomposition of these complexes must occur before the polymer film can interact strongly with the substrate [7]. PAA solutions are capable of strong interaction with the substrate. When PAA films are spin coated onto copper substrates from solutions in NMP, the PAA etches the oxide on the surface of the substrate and copper ions are found in the polymer films a distance of several micrometers from the substrate surface. This increases the dielectric constant of the films and substantially alters their mechanical properties [8].

Many of these issues can be eliminated by using a solvent-free technique which involves vapor deposition of PMDA and ODA monomers onto a substrate under vacuum [9]. The monomers react rapidly during deposition to form polyamic acid, which may be thermally or chemically imidized. Films deposited in this manner fill small features better than spin coated films, but tend to follow the surface topology and do not planarize the surface as well as spin coated films [7, 10].

Several authors have investigated the vapor deposition of ultrathin films of PMDA and ODA monomers onto various substrates [11-16]. PMDA appears to chemisorb onto silver and copper as a bidentate carboxylate salt [11, 15]. ODA monomer has been reported to fragment during adsorption onto silver [11]. It has also been reported that ODA physisorbs onto copper and silver surfaces [15, 16].

Other workers have described the vapor deposition of thick films onto silver surfaces [17]. Analysis with Raman spectroscopy suggested that the films were deposited as polyamic acid with a slight amount of ring closure to the imide structure. Heating at 200°C for 30 minutes resulted in films that were completely imidized and were spectroscopically identical to films of spin-coated PMDA/ODA.

Previous work also suggested that the *bulk* structure of vapor-deposited polyimides was very similar to that of spin-coated materials and that the qualitative adhesion to silicon was excellent [9]. However, the relationship between *interfacial* structure and the adhesion of vapor-deposited polyimide films to silicon and other substrates has not been reported.

Langmuir-Blodgett (LB) films for electronic and optical device applications have also attracted interest, largely due to the fact that ordered uniform LB films can be made with very precise control of structure and thickness. Kakimoto and co-workers [18, 19] reported the first successful preparation of monolayer films of PMDA/ODA polyimide using the LB technique. Since the polyamic acid of PMDA/ODA has only hydrophilic carboxyl groups in the polymer backbone and does not form a stable Langmuir film at the air-water interface, these authors proposed a "precursor method." A monolayer film of polyamic acid alkylamine salt was prepared at the air-water interface and deposited onto a substrate by the LB technique. Subsequently, the LB film of polyamic acid alkylamine salt was converted into a monolayer film of polyimide by thermally or chemically removing the long alkyl chain. Studies using scanning tunneling microscopy [20-22] and atomic force microscopy [23,24] showed the polymer chains were aligned parallel to the deposition direction. However, the interfacial structure as well as the orientation of the pyromellitic diimide and diphenyl ether moieties, which may be regarded as the building blocks of PMDA/ODA polyimide, are still under debate.

Adhesion promoters based on silane chemistry can be used to improve polymer/metal adhesion. Silane coupling agents have the general structure $X_3Si\text{-}R\text{-}Y$, where Y is an organofunctional group selected for bonding to specific organic polymers and X is a hydrolyzable group which forms silanol (SiOH) groups in aqueous solutions. Silanol groups are thought to be capable of reacting with mineral hydroxides (MOH) through hydrogen bonding or through condensation to form oxane (SiOM) bonds. The combination of strong, stable bonds between the polymer and the organofunctional groups and between the substrates and silanol groups improves the strength and durability of interfaces significantly.

Silanes are used extensively for improving adhesion of polyimides to various inorganic substrates [25 and references therein]. In particular, γ-aminopropyltriethoxysilane (γ-APS) is used frequently as an adhesion promoting primer for SiO_2/polymide interfaces. The mechanism by which aminosilanes enhance adhesion between SiO_2 and polyimides appears to involve formation of imide linkages between the polyamic acid and the primary amine of the adhesion promoter [26]. Although this must result in chain scission of the amic acid during ring closure, the strength and hydrothermal stability of these interfaces is significantly improved over that obtained from unsilanted surfaces.

Aminosilane is an excellent adhesion promoter for aluminum/epoxy interfaces [27] where it inhibits corrosion of the aluminum substrate during environmental aging. In this investigation, γ-APS was used to chemically modify the substrate surface and its effect on both interfacial structure and interfacial fracture energy in the PMDA/ODA polyimide/aluminum system was determined.

Adhesion between spin-coated films and rigid substrates is frequently measured using a 90° peel test [28, 29]. However, because of the bending and stress concentrations that occur in the polymer films during debonding, well over half of the energy expended in a peel test can be dissipated as heat and/or stored in the polymer as residual strain energy [30]. Only in certain cases [31, 32] is this test useful for determining the true adhesive fracture energy (G_a).

Gent and Lewandowski [33] proposed a circular "blister test" to quantify the interfacial fracture energy between deformable polymeric films and rigid substrates. The test specimen

consists of a rigid substrate with a thin flexible overlayer. A fluid is injected at the interface through a central perforation in the substrate. The strain energy stored as elastic deformation of the overlayer is given by

$$G = 0.649\,Py \tag{1}$$

where P is the pressure and y is the blister height. This energy is available to propagate a crack at the interface. When the pressure is increased beyond a critical value (P_c), the blister begins to grow. This critical pressure defines the critical strain energy release rate (G_a) for the interface. The amount of plastic deformation that occurs in this test is less than for the 90° peel test, largely because the angle between the polymer film and the substrate at the crack front is very low. However, the amount of plastic deformation that occurs on a global scale in a blister test can still be significant for tough, well adhered films such as polyimides on aluminum. To account for this, data obtained from several samples was analyzed using a finite element model for the circular blister test. This analysis allowed partitioning of the total strain energy release rate into components due to global plastic deformation and to other processes, including adhesion. The results gave insight into the nature of the mechanical properties of the interphase region where failure occurred.

This report describes our work on adhesion of thin polyimide films to metal substrates. Films were deposited onto the substrates using spin-coating, vapor deposition, and Langmuir-Blodgett techniques. The structure and composition of the films were probed using X-ray photoelectron spectroscopy (XPS), surface-enhanced Raman spectroscopy (SERS), and reflection-absorption infrared spectroscopy (RAIR). Interfacial fracture energies (G_a) were measured using a circular blister test. Finally, we related the various interface structures to the interfacial fracture energy of polyimide/metal bonds. This work provided a clear relationship between the structure and mechanical properties of the interphase as it relates to the substrate chemistry and deposition technique.

II. Experimental

Three different polyamic acids were obtained from Dupont Corp. They included PMDA/ODA, PMDA/4-BDAF, and 6FDA/ODA. 4-BDAF is 2,2'-bis[4-(4-aminophen-oxy)phenyl]-hexafluoropropane while 6FDA is 2,2-bis(3,4-dicarboxyphenyl)-hexafluoropropane.

Silver substrates were prepared for SERS and RAIR investigations by evaporation of the metal onto clean glass slides. The slides were immersed in chromic-sulfuric acid overnight and then in 0.1 N NaOH solutions for 1 hour. They were then rinsed in distilled-deionized water, blown dry with nitrogen, cleaned ultrasonically in absolute ethanol several times, and again blown dry with nitrogen. The slides were then placed in a vacuum chamber, purged with nitrogen, and pumped down to approximately 10^{-6} Torr using a combination of sorption, sublimation, and ion pumps. High purity silver wires (99.99%, Aldrich) which had been wrapped around a tungsten filament were resistively heated to evaporate the silver and deposit films onto the glass slides. The film thickness and the deposition rate were controlled using a quartz crystal oscillator thickness monitor. Films with a thickness of approximately 40 Å or 1,000 Å were prepared for SERS and RAIR, respectively. Gold substrates for RAIR and SERS were prepared in a similar manner.

Aluminum substrates for RAIR and XPS investigations were prepared by mechanical polishing. These substrates were degreased in acetone, ground on wet SiC paper, and then polished using 6 μm and 1 μm diamond compounds. The substrates were cleaned ultrasonically, first in ethanol and then acetone, and finally etched in an oxygen plasma for 10 minutes in a microwave reactor using 200 watts of power, 45 sccm flow rate of oxygen, and 500 mTorr pressure.

LB films of PMDA/ODA polyimide were deposited onto silver substrates as follows. A solution of polyamic acid alkylamine salt in a mixture of NMP and benzene (concentration of 1 mmol/l) was prepared from the polyamic acid of PMDA/ODA and dimethylhexadecylamine (98%, Pfaltz & Bauer, Inc.) in a 1:2 molar ratio just before deposition. Solutions of the polyamic acid alkylamine salt were then spread onto a pure deionized distilled water subphase (resistivity of 18 MΩ cm at room temperature). The films were compressed in a film balance (Nima 622D2 trough) to the deposition pressure of 25 mN/m. Transfer of the monolayer films to silver substrates supported on glass slides was carried out by raising and lowering the slides through the air-water interface at a rate of 10 mm/min. As-deposited LB films were converted to polyimide by heating at 200°C for 1 hr under nitrogen. However, the morphology of the silver island films used as substrates for SERS was unstable at the relatively high temperatures required for imidization. Therefore, chemical imidization was used for SERS experiments.

4-Mercaptophenylphthalimide (4-MPP) was synthesized as follows. Equimolar amounts of phthalic anhydride and 4-aminothiophenol were mixed together in N,N-dimethylacetamide. The mixture was refluxed overnight at a temperature of 160°C under nitrogen and then cooled to room temperature. The pale yellow precipitate which formed was filtered, rinsed with copious amounts of ether, and dried under vacuum at 75°C for several hours.

Monolayers of 4-MPP were prepared by immersing a gold substrate into a 10^{-3} M solution of 4-MPP in chloroform for 12 hours. Afterwards, the samples were rinsed thoroughly with chloroform.

Thin films of the polyamic acids of 6FDA/ODA and PMDA/4-BDAF used in spectroscopic studies were deposited onto aluminum substrates by spin-coating from solutions in N-methylpyrrolidone (NMP). The films were heated at 100°C for 30 min to remove the solvent and then heated at 200°C under nitrogen for an additional 30 min to convert the PAA to the corresponding polyimide.

Vapor deposition of PMDA and ODA onto aluminum was carried out in a modified diffusion-pumped NRC thermal evaporator (see Figure 1). Monomers were sublimed from independently heated aluminum crucibles. The evaporation crucibles were contained within a cylindrical aluminum baffle, equipped with a heater to prevent condensation of the vaporized monomer on its surface. The target substrate was suspended about 1 cm above the cylindrical baffle. Both the crucibles and the substrate base were equipped with chilled water cooling. This helped improve the rate of condensation on the substrate during deposition and allowed for rapid cool-down of the monomer crucibles at the end of a deposition cycle. Temperatures of the crucibles, baffles, and substrate were controlled by closed-loop PID temperature controllers. System pressure during deposition was around 5×10^{-6} torr as measured with an ionization gauge

located on the bell jar baseplate remote from the cylindrical baffle. The films were analyzed as-deposited or after thermal imidization in a nitrogen atmosphere.

Samples for blister testing were prepared from aluminum disks having a diameter of 101.6 mm and thickness of 25.4 mm. A hole was drilled at the center of the substrate and threaded. The substrate was then mechanically polished as described previously. The hole in the substrate was plugged with a thin disk of KBr formed *in-situ.*and the substrate was cleaned in an oxygen plasma as described above. Polyimide films were deposited onto the substrates by spin-coating a solution of polyamic acid. These films were converted to polyimide by heating at 100°C for 1 hr and at 200°C for 1 hr in nitrogen.

Some aluminum substrates were silanated before the polyamic acid was spin-coated. After plasma cleaning, these substrates were immersed in a 1% aqueous solution of γ-aminopropyltriethoxysilane (γ-APS) for 10 sec, removed from the solution, blown dry using nitrogen gas, and dried under vacuum at 85°C for 10 min. A film of the polyamic acid of PMDA/ODA was then spin-coated onto the substrates and imidized as described above.

In some cases, vapor-deposited films of PMDA/ODA polyamic acid were applied to the substrates and thermally imidized. These films were too thin for blister testing, so thicker films of PMDA/ODA polyamic acid were spin-coated on top of them and imidized. Prior to applying the overlayer, the vapor-deposited films were treated in an oxygen plasma to ensure adhesion of spin-coated polyimide. This procedure resulted in composite films with identical bulk mechanical properties to spin-coated films, but with a metal/polymer interface that consisted of vapor-deposited polyimide.

Gold substrates for blister testing were prepared in a similar manner. A hole was drilled at the center of a steel substrate having a diameter of 101.6 mm and thickness of 25.4 mm. The hole was threaded and the substrate was mechanically polished and then cleaned ultrasonically in acetone. Gold films having a thickness of ~0.2 μm were electroplated onto the substrates at Smith Electrochemical (Cincinnati, OH) and the hole was plugged with a KBr disk. The gold-plated substrates were etched in an oxygen plasma as described above and thin films of polyamic acid were applied by spin coating. The PAA films were then converted to the polyimide by heating at 100°C for 1 hr and at 200°C for 1 hr.

Two different set-ups were used for blister testing. One consisted of a syringe pump, pressure transducer, video camera, frame grabber, and computer and was constructed at the University of Cincinnati (see Figure 2). After dissolving the KBr disc with water, the substrate was connected to the blister testing apparatus by threading a fitting into the hole in the substrate. The film was then pressurized at a constant flow rate of 0.3 ml/min using water as the pressurizing medium. At appropriate intervals, the pressure was recorded and a video image of the blister was stored. Blister height and radius were measured from the stored image and correlated with the applied pressure. When the blister just began to grow, the critical pressure P_c and the height of the blister y were determined and equation 1 was used to determine G_a. After delamination, the polymer and substrate failure surfaces were analyzed using XPS and RAIR.

The other set-up was located in the laboratories of Prof. K. M. Liechti at the University of Texas at Austin and was similar except that a grid was projected onto the film and a video camera was used to continuously record the full three-dimensional shape of the blister as the

pressure was increased up to and beyond the point at which the blister began to grow. The shape of the blister was then analyzed using finite element analysis so that the total fracture energy and the energy dissipated in global plastic deformation could be determined.

SERS spectra were obtained using a Raman spectrometer consisting of a Spex 1401 double monochromator, Hamamatsu R943-02 photomultiplier, Stanford Research Model 400 gated photon counter interfaced to a Hewlett-Packard Vectra computer, Spectra-Physics Model 165 argon-ion laser, and Lexel 3000 krypton ion laser. Spectral resolution was approximately 10 cm^{-1} for the SERS spectra. The angle between the laser (s-polarized, power ranging from 10 to 30 mW) and the sample was about 60° relative to the sample normal. The green line of the argon ion laser (514.5 nm) was used to excite SERS spectra of thin films on silver substrates while the red line of the krypton ion laser (647.1 nm) was used for films on gold substrates. Scattered light was collected using an f/0.95 collection lens and focused onto the entrance slits of the monochromator. Spectra were obtained using a scan speed of 1 cm^{-1} per second. Plasma lines were removed from the spectra by placing a narrow-bandpass filter between the laser and sample. Normal Raman spectra were acquired using the same instrument and instrumental parameters but with 5 cm^{-1} resolution.

RAIR spectra were obtained using a Perkin-Elmer Model 1800 Fourier-transform infrared (FTIR) spectrometer and external reflection accessories provided by Harrick Scientific. One reflection at 78° was used in all cases. Spectra were collected at 4 cm^{-1} resolution and between two hundred and five hundred scans were averaged for each spectrum. All RAIR spectra reported here are difference spectra obtained by subtracting spectra of baselines (substrates) from spectra of film-covered substrates.

Transmission infrared spectra were obtained using the spectrometer described above. Samples were prepared by placing a small amount of the compound onto potassium bromide (KBr) pellets. Polyamic acids were thermally imidized by heating the film-covered pellets at 200°C for 60 minutes.

Infrared micro-spectroscopy was used to characterize the aluminum failure surfaces of blister test specimens prepared from silanated substrates. Spectra were collected at a resolution of 4 cm^{-1} using a Nicolet Nic-Plan microscope with grazing angle objective which was interfaced to a Nicolet Magna 760 optical bench. Five hundred scans were averaged for each spectrum.

XPS spectra were obtained using a Physical Electronics Model 5300 X-ray photoelectron spectrometer with Mg Kα radiation at a power of 300 W. The pass energy was 44.75 eV (0.5-eV step; 25-ms dwell time per step) and 17.90 (0.05-eV step; 50-ms dwell time per step) for the survey and high-resolution spectra, respectively. During analysis, the pressure was kept at 10^{-8} to 10^{-9} Torr. A take-off angle of 45° was used to obtain all spectra. The XPS spectra were corrected for charging by referencing the aliphatic C(1s) peak to 284.6 eV. Elemental compositions of the various surfaces were determined by integration of the areas under the individual elemental peaks in the high-resolution spectra. The spectra were fitted using a 90%/10% Gaussian/Lorentzian peak shape.

The thickness of the films was determined by using a Rudolph Research Model 436 ellipsometer to examine the metal substrates before and after deposition of the films. A

computer program developed by McCrackin [34] was used to compute the film thickness from the ellipsometry parameters Δ and ψ.

III. Results and Discussion

A. Characterization of Interfaces between 6FDA/ODA Polyimide and Aluminum

RAIR spectra obtained from films of polyamic acid spin-coated onto aluminum substrates from 4%, 1.6%, 0.8%, 0.4%, 0.2% and 0.1% solutions in N-methylpyrrolidone (NMP) are shown in Figure 3. The thickness of these films (determined by ellipsometry) was about 550, 200, 100, 60, 30, and 15 Å. As the thickness of the films decreased, the relative intensity of the band near 1724 cm^{-1} due to the C=O stretching mode of the acid groups decreased while the intensity of the broad band near 1650 cm^{-1} increased. While this band includes contributions from both amide and aluminum carboxylate modes, the increase in intensity of this band as the film thickness decreased was probably due to increased contribution from the carboxylate groups formed at the aluminum surface. This was consistent with the decrease in the intensity of acid C=O stretching band near 1724 cm^{-1}.

The RAIR spectra of these films after imidization under nitrogen at 100°C for 30 minutes and at 200°C for an additional 30 minutes are shown in Figure 4. Significant differences were observed in the spectra as the film thickness decreased. Spectra obtained from the thicker films (Figures 4A-4C) were dominated by strong bands near 1735 and 1380 cm^{-1} which were assigned to the imide C=O and CNC symmetric stretching modes, respectively. This showed that the bulk of the polyamic acid films had been converted to the corresponding polyimide. However, as the thickness of the films decreased, the imide bands near 1730 and 1380 cm^{-1} became weaker, while the band near 1650 cm^{-1}, which was attributed to carboxylate salt, became stronger. The effects of thickness on the RAIR spectra were especially significant for the thinnest films (Figure 4F). In that case, imide bands near 1730 and 1380 cm^{-1} were almost non-existent, while the bands characteristic of carboxylate groups near 1650 cm^{-1} were quite strong. These results indicated that formation of aluminum carboxylates in the interphase inhibited imidization.

The relative band intensities in grazing angle RAIR spectra are sensitive probes of the molecular orientation in the Z direction (parallel to the surface normal). The relative intensities of bands in the RAIR spectra of relatively thick films (Figures 4A-4C) were very similar to those in the transmission infrared spectrum of 6FDA-ODA polyimide [35]. This implied that the bulk polyimide films were randomly oriented, at least in the Z direction. However, evidence of preferred orientation of the carboxylate that formed close to the metal oxide surface was observed. The dipole moment of the asymmetric carboxylate stretching mode (near 1650 cm^{-1}) has a component perpendicular to the long axis of the molecule, while the dipole moment of the symmetric carboxylate stretching mode (near 1410 cm^{-1}) is parallel to this molecular axis. The band due to the symmetric mode was always significantly weaker than that assigned to the asymmetric mode (see Figures 4E and 4F). This implied that the long axis of the 6FDA carboxylate species was mostly parallel to the oxide surface, and that the plane of the carboxylate groups formed a non-zero angle with the surface normal.

It is also interesting to note that the intensity of the band near 1502 cm^{-1}, which was assigned to the tangential ring stretching mode ν(19a) of the C_6H_4 rings of ODA, was substantially stronger in the spectra of the spin coated films on aluminum substrates than in

transmission IR spectra [20]. This suggested that the ODA moieties were deposited so that the edge of the plane was oriented toward the oxide surface.

XPS spectra obtained from spin-coated 6FDA/ODA polyamic acid on aluminum substrates provided additional evidence of carboxylate formation. Figures 5 and 6 show high-resolution C(1s) spectra obtained from films deposited from 0.2% solution in NMP before and after imidization. The C(1s) spectrum of the thin PAA film on aluminum before imidization was similar to that for the bulk PAA [35]. However, the component due to acid groups (4.2 eV shift) was somewhat weaker and the component due to amide and carboxylate (3.3 eV shift) was stronger. These results were consistent with those from RAIR spectroscopy and supported the conclusion that some acid groups of PAA reacted with aluminum to form carboxylates.

Heating these PAA films to 200°C for 30 minutes resulted in little change in the XPS spectra, showing that imidization was inhibited by the formation of aluminum carboxylate species. The C(1s) spectrum of the film after heating (Figure 6) was more similar to the polyamic acid spectrum than to the spectrum of the bulk 6FDA/ODA polyimide [35], and the component shifted 3.3 eV from the aliphatic carbon peak at 284.6 eV, which was assigned to amide and carboxylate moieties, was still strong.

After heating, a minor component shifted 4.1 eV from the main C(1s) peak characteristic of imide groups was observed, indicating partial imidization. The peak at a shift of 1.0 eV, attributed to C-N species of ODA and the aromatic ring carbons of the 6FDA [36], also increased in intensity.

Inhibition of imidization by interaction of the polyamic acid with aluminum was further evidenced by the high-resolution N(1s) spectra. Only one peak near 400.0 eV, which was due to the amide groups, was observed before curing. However, the N(1s) spectra obtained after curing were readily resolved into two components, a stronger peak near 400.3 eV due to amide species and a minor component near 401.1 eV characteristic of the imide form. Thus, both XPS and RAIR results indicated that curing of the polyamic acid of 6FDA/ODA was inhibited by formation of aluminum carboxylates.

B. Characterization of Interfaces between PMDA/4-BDAF Polyimide and Aluminum

RAIR and XPS were used to investigate the interphase formed when thin films of PMDA/4-BDAF polyamic acid were imidized against aluminum substrates. RAIR spectra obtained from films of polyamic acid spin-coated onto aluminum substrates from 2.5%, 0.8%, 0.2%, and 0.1% solutions in N-methylpyrrolidone (NMP) are shown in Figure 7. The thickness of these films was about 350, 100, 40, and 20 Å, respectively. As was the case with the 6FDA/ODA polymers, the band near 1724 cm^{-1}, assigned to the C=O stretching mode of the polyamic acid, became weaker and the bands near 1650 cm^{-1} assigned to amide and carboxylate became stronger as the thickness of the films decreased. Acid groups close to the interface had been converted to carboxylate through interaction with the aluminum oxide.

RAIR spectra obtained from these films after thermal treatment are shown in Figure 8. The bands near 1730 and 1380 cm^{-1}, which were related to C=O and axial CNC stretching modes of imide groups, became weaker as the film thickness decreased, while the band near1650 cm^{-1} due to the asymmetric carboxylate stretching mode became stronger. The band near 1502 cm^{-1} (tangential ring stretching mode ν(19a) of the C_6H_4 rings) and the band near 1250 cm^{-1} (COC and

CF_3 asymmetric stretching) remained strong. These results indicated that imidization of the polyamic acid was inhibited by formation of aluminum carboxylates in the interphase region. Since the infrared spectra obtained from thin films of 6FDA/ODA and PMDA/4-BDAF were nearly identical, it was concluded that these materials behaved similarly on aluminum substrates.

High-resolution C(1s) spectra obtained from thin films of polyamic acid of PMDA/4-BDAF spin-coated onto aluminum substrates from a 0.2% solution in NMP before and after imidization are shown in Figures 9 and 10, respectively. The overall line shapes of the high-resolution C(1s) spectra for thin polyamic acid films deposited onto aluminum substrates were similar to those for bulk polyamic acid [37]. However, because of the similar electron withdrawing effects of amide and carboxylate groups on carbon, the component shifted 3.3 eV from the main carbon peak at 284.6 eV contained contributions from both the amide and carboxylate functionalities.

After heating, the C(1s) spectra of the thin films were more similar to those of the polyamic acid before imidization than to those of the bulk PMDA/4-BDAF polyimide [37], showing that imidization of polyamic acid was inhibited by formation of aluminum carboxylates. This was confirmed by the peak due to amide and carboxylate groups located about 3.2 eV from the main C(1s) peak.

A weak component 4.1 eV from the main peak which was characteristic of imide groups, indicated that at least partial imidization of the polyamic acid did, however, occur. The peak at a separation of 1.0 eV, which was attributed to C-N and aromatic carbon of PMDA moieties, also increased in intensity.

Additional evidence that imidization was inhibited by interaction of the polyamic acid with aluminum was provided by the high-resolution N(1s) spectra. A single peak due to amide nitrogen was observed near 400.2 eV in the N(1s) spectrum of polyamic acid films. After imidization, two components were observed in the N(1s) spectrum. The main component, near 400.4 eV, was only 0.2 eV higher than than for the polyamic acid, again indicating that imidization had been inhibited. Overall, both the XPS and RAIR results indicated that imidization of the polyamic acid of PMDA/4-BDAF in the interphase was inhibited by formation of aluminum carboxylates.

C. Characterization of Interfaces between Langmuir-Blodgett Films of PMDA/ODA and Silver [38]

RAIR spectra obtained by transferring 1-layer and 3-layers of the PMDA/ODA polyamic acid dimethylhexadecylamine salt to silver substrates are shown in Figure 11. The thickness of these films was about 11 and 34 Å, respectively, indicating transfer in a layer-by-layer manner. The linear increase of the absorbance as a function of the number of layers further demonstrated that the LB film actually transferred to the silver substrates in a layer-by-layer fashion.

SERS spectra obtained from 1-layer and 3-layer LB films on silver are shown in Figure 12. The strong band near 1410 cm^{-1} in SERS spectra was attributed to the symmetric carboxylate stretching mode. This assignment was supported by the observation of a strong band near 1620 cm^{-1} and a weak band near 860 cm^{-1} in the SERS spectrum of the salt. The strong band near 1620 cm^{-1} was attributed to a combination of the tangential stretching modes of benzene rings and the asymmetric stretching mode of carboxylate groups. The band near 860 cm^{-1} was assigned to the

deformation mode of carboxylate groups. The strong intensity of this band indicated that the as-prepared LB films were indeed deposited onto silver substrates mainly as salts, not free acid.

SERS spectra of the 1-layer and 3-layer salt LB films after imidization are shown in Figure 13. It was evident from the appearance of strong bands near 1800, 1700, and 1400 cm^{-1} in the SERS spectra that imidization was quite complete. These bands were assigned to the carbonyl stretching mode of the imide, carbonyl stretching of isoimide, and to the axial C-N-C stretching mode, respectively. The formation of significant isoimide species resulted from the chemical imidization process, which produces much more isoimide than does the thermal imidization process [39].

RAIR spectra obtained after imidizing polyamic acid alkylamine salt films are shown in Figure 14. The RAIR spectra again indicated that the imidization was quite complete as evident from the strong band at 1730 cm^{-1} assigned to the C=O stretching mode of the imide. RAIR results also indicated orientation induced by imidization. For example, the bands near 1500, 1380, and 1240 cm^{-1} were much weaker than the band near 1730 cm^{-1} even though they have nearly the same intensity in transmission infrared spectra. Assuming an edge-on orientation for the PMDA moieties, the band near 1730 cm^{-1} would have a stronger intensity than the band near 1380 cm^{-1}, since the transition moment for the C=O stretching mode would be perpendicular to the surface and that for the axial C-N-C stretching mode assigned to the band at 1380 cm^{-1} would be parallel. The weak bands near 1500 and 1240 cm^{-1} suggested that the ODA moieties were more parallel to the surface than in as-deposited LB films. The orientation of polyimide LB films observed here was very similar to that of spin-coated films [40], indicating that preferential orientation may have accompanied the imidization process.

SERS and RAIR results indicated that on silver substrates, films of acid salts deposited by LB techniques imidized more readily than spin-coated films of polyamic acid. Strong interactions seen between spin-coated films and the silver substrate were not seen in the LB films. The acid form of the carboxyl groups reacted readily with the silver to form carboxylate salts which inhibited imidization. The presence of solvent during the spin-coating process also facilitated formation of carboxylate salts by increasing the mobility of the polyamic acid near the interface.

It is well known that RAIR spectroscopy can be used for quantitative determination of the preferred orientation of molecules adsorbed onto reflective surfaces. Bands corresponding to vibrational modes having transition moments perpendicular to the substrate appear with enhanced intensity in RAIR spectra, while those with transition moments parallel to the surface appear with reduced intensity. The band intensities are thus orientation-dependent and can give information about the tilt and rotation angles of molecules adsorbed on metal substrates.

Let us define laboratory coordinates so that z is the direction perpendicular to the metal surface, while x and y represent directions in the plane parallel to the surface. The angle between the long axis of the adsorbed molecules and the z coordinate is then defined as θ (*i.e.*, tilt angle of the long molecular axis away from the surface normal). ϕ is the angle between the molecular plane and the x-z plane (*i.e.*, rotation angle of the molecule about the long molecular axis). By calculating the intensity ratios of selected bands in RAIR and transmission IR spectra, θ and ϕ can be obtained using equations (2) and (3)

$$A_{||}(R)/A^{i}_{\perp}(R) = [A_{||}(T)/A^{i}_{\perp}(T)]\ [\cot^2\theta/\cos^2\phi] \quad (2)$$

$$A_{||}(R)/A^{o}_{\perp}(R) = [A_{||}(T)/A^{o}_{\perp}(T)]\ [\cot^2\theta/\sin^2\phi] \quad (3)$$

where

$A_{||}(R)$ - absorbance of a band in RAIR spectra having the dipole moment parallel to the long molecular axis,

$A^{i}_{\perp}(R)$ - absorbance of a band in RAIR spectra having the dipole moment perpendicular to the long molecular axis and in the molecular plane,

$A^{o}_{\perp}(R)$ - absorbance of a band in RAIR spectra having the dipole moment perpendicular to the long molecular axis but out of the molecular plane,

$A_{||}(T)$ - absorbance of a band in the transmission IR spectra (isotropic spectra) having the dipole moment parallel to the long molecular axis,

$A^{i}_{\perp}(T)$ - absorbance of a band in the transmission IR spectra (isotropic spectra) having the dipole moment perpendicular to the long molecular axis and in the molecular plane, and

$A^{o}_{\perp}(T)$ - absorbance of a band in the transmission IR spectra (isotropic spectra) having the dipole moment perpendicular to the long molecular axis but out of the molecular plane.

In this work, bands near 1730, 1380, and 726 cm^{-1} were selected to determine the orientation of the PMDA moieties in the LB films. The dipole moment of the imide C=O stretching mode near 1730 cm^{-1} is perpendicular to the long molecular axis and is in the molecular plane of the PMDA. The dipole moment of the imide C-N-C stretching mode near 1380 cm^{-1} is parallel to the long molecular axis. The band near 726 cm^{-1}, which was attributed to the C-N-C out-of-plane vibrational mode, has a dipole moment mostly perpendicular to the long molecular axis but out of the molecular plane. The absorbance of these bands was measured using a tangent-line method. The tilt and rotation angles were then calculated using equations 2 and 3. The tilt and rotation angles of the 1-layer LB polyimide film were 67° and 28°, respectively. The tilt and rotation angles of 3-layer films were 69° and 29°, respectively. These results indicated that the axis of PMDA moieties tilted away from the surface normal about 70°. In other words, the long molecular axis was nearly parallel to the silver surface. The plane of PMDA moieties was almost perpendicular to the silver surface. These values were in good agreement with the conclusions drawn from the qualitative analysis.

LB polyimide films were also studied using XPS. High-resolution C(1s) spectra obtained before and after imidization of the alkylamine salt precursor films are shown in Figures 15 and 16. Extensive imidization of the LB films was evident from the presence of a strong component at 4.0 eV shift (imide) and the strong peak at a 1.1 eV shift (aromatic carbons in PMDA and C-N bonds).

D. Characterization of 4-MPP films on gold substrates [41,42]

The normal Raman spectrum obtained from neat 4-MPP is shown in Figure 17. Strong bands were observed near 1789 and 1717 cm^{-1} and assigned to the symmetric and asymmetric stretching modes of the imide carbonyl groups, respectively. The band near 1395 cm^{-1} was assigned to the CNC axial stretching mode. The medium intensity band near 2581 cm^{-1} and the

weak band near 915 cm^{-1} were assigned to the stretching and bending modes of S-H groups, respectively. Most of the remaining bands were assigned to modes of the para- and ortho-disubstituted rings.

Figure 18 shows the SERS spectrum of 4-MPP adsorbed onto a gold substrate. Significant differences were observed when the SERS and normal Raman spectra were compared. The band near 2581 cm^{-1} was not observed in the SERS spectra, indicating that dissociation of the S-H bonds occurred during adsorption. Other bands shifted in position after adsorption, including those near 1604 and 1100 cm^{-1} in the normal Raman spectra, providing support to the concept of chemisorption.

The transmission infrared spectrum of 4-MPP is shown in Figure 19. Between 600 and 2000 cm^{-1}, the spectrum was dominated by bands related to imide vibrations. For example, bands near 1782, 1710, 1388, 1121, and 717 cm^{-1} were assigned to the symmetric C=O stretching, asymmetric C=O stretching, CNC axial stretching, CNC transverse stretching, and CNC out-of-plane bending modes, respectively. Bands near 2572 and 908 cm^{-1} were assigned to the S-H stretching and bending modes, respectively.

Figure 20 shows the RAIR spectrum of a 4-MPP monolayer adsorbed onto a gold substrate. The disappearance of the bands near 2572 and 908 cm^{-1} again indicated that 4-MPP was chemisorbed through the S-H groups.

Equations 2 and 3 were used to determine the tilt and rotation angles for 4-MPP adsorbed onto gold. In order to do so, it was necessary to choose two pairs of bands such that the dipole moments of the bands in each pair were perpendicular to each other (one parallel to the molecular axis, the other perpendicular to it). In this investigation, the bands near 1388, 1710, and 717 cm^{-1} were selected. It was found that the tilt angle was about 21° while the rotation angle was 42°. A tilt angle of 21° indicated that the molecular axis of 4-MPP was nearly perpendicular to the gold surface. The rotation angle of 42° was close to the average value of 45°, probably indicating that there was no preferred rotational orientation for the imide groups. These results were in excellent agreement with those obtained from a molecular dynamics simulation of the adsorption of 4-MPP onto gold.

E. Characterization of the Interface Between PMDA/ODA Polyimides and Aluminum

1. Spin-coated polyimide films on aluminum

The RAIR spectrum obtained from a thin film which was prepared by spin-coating the PMDA/ODA polyamic acid onto aluminum substrates from a 0.2% solution in NMP and then heating at 100°C to drive off the solvent is shown in Figure 21A. Ellipsometry indicated that the thickness of this film was ~35 Å. The broad band near 1650 cm^{-1} contained contributions from amide, carboxylate, and aromatic ring modes while the band near 1410 cm^{-1} was a combination of the COH in-plane bending mode of acid groups and the symmetric stretching mode of carboxylate groups. However, the band near 1724 cm^{-1}, which was characteristic of the C=O stretching mode of the acid groups, was almost non-existent. These results demonstrated the formation of carboxylate salts at the interface by reaction between polyamic acid and the aluminum substrate.

When this film was heated at 200°C for 1 hour under nitrogen, new bands characteristic of imide groups were found near 1785, 1727, and 1376 cm^{-1} (see Figure 21B). Bands near 1785 and 1727 cm^{-1} were assigned to imide C=O stretching modes. The band near 1376 cm^{-1} was attributed to the axial C-N-C stretching mode of imide. Appearance of these bands due to imide species showed that significant imidization occurred as a result of thermal treatment. However, the strong, broad band near 1610 cm^{-1}, which was attributed to aluminum carboxylate salt, indicated that imidization was incomplete at the interface region. This is similar to the results obtained by other workers on reactive metal substrates such as copper or silver [43-46] where carboxylate formation between the polyamic acid and metal oxide resulted in inhibition of the imidization reaction.

2. Vapor-deposited polyimide films on aluminum

Deposition of polyimides by condensation from the vapor phase is a process that is distinct from solution deposition or LB deposition in several important ways. During vapor phase deposition, reaction between anhydride and amine monomers does not occur until the monomers have condensed onto the substrate. Therefore the adsorption process (and the subsequent polymerization and adhesion) depends on the interaction of the monomers with the surface. Adsorption of low molecular weight amines and anhydrides can differ significantly from that of a polyamic acid. In addition, there is no solvent present to provide mobility for the monomers, to compete with the monomers for adsorption sites [47], or to provide mobility for metal particles to migrate into the polymer film [48].

The investigation of the vapor deposition process began with vapor deposition of the individual monomers to look for evidence of interaction between the monomers and the surface that was distinct from the corresponding moieties in spin-coated or LB films.

a. Vapor-deposited PMDA

The RAIR spectrum of a vapor deposited PMDA film with a film thickness of 30 Å on an aluminum is shown in Figure 22. Bands near 1850 and 1780 cm^{-1} were assigned to the symmetric and asymmetric stretching C=O stretching modes of PMDA monomer. A band near 1260 cm^{-1} was assigned to the COC stretching mode. The strong, broad band near 1600 cm^{-1} (asymmetric carboxylate stretching mode) clearly showed that PMDA vapor reacted with aluminum to form carboxylate salt, similar to those seen in the spin coated films of polyamic acid. The relative amount of the carboxylate formed during vapor deposition was variable, however.

b. Vapor-deposited ODA

A RAIR spectrum of a 40 Å thick ODA film vapor deposited onto an aluminum substrate is shown in Figure 23. The bands near 1620 and 1500 cm^{-1} were assigned to $\nu(8a)C_6H_4$ and $\nu(19a)C_6H_4$ ring modes, respectively while the band near 1230 cm^{-1} was assigned to the C-O-C stretching mode. No additional bands related to the chemisorbed species were observed, and the spectrum was very similar to the transmission IR spectrum of ODA. These results indicated that vapor deposited ODA physisorbed onto aluminum oxide without significant chemical interaction. Dissociative chemisorption of ODA onto silver in vapor deposited films has been reported by other workers [49,50], but was not observed here on aluminum substrates.

c. Co-deposited PMDA and ODA

RAIR and XPS were used to study a vapor deposited film of PMDA/ODA on aluminum which had a film thickness on the order of 30 Å. The RAIR spectrum of the film as-deposited is shown in Figure 24A. Bands near 1850 and 1780 cm^{-1} were assigned to the anhydride C=O stretching and asymmetric stretching modes of unreacted PMDA monomer, respectively. The strong band near 1500 cm^{-1} was due to the C-C stretching mode ν(19a) of the C_6H_4 rings. The band near 1240 cm^{-1} was assigned to the COC stretching mode. Bands near 1663 and 1542 cm^{-1} were attributed to the C=O stretching and N-H bending modes of amide groups, indicating that some polyamic acid was formed in the co-deposited monomer film. This was further supported by the observation of a band near 1720 cm^{-1} due to the acid C=O stretching mode. However, the broad band centered near 1610 cm^{-1} showed that carboxylate salts were present.

When the film was thermally imidized (Figure 24B), the band near 1610 cm^{-1} due to aluminum carboxylate salts remained significant, indicating that at least some inhibition of imidization had occurred. The amount of carboxylate formation in the thin vapor deposited films was somewhat variable, but generally less than seen in the spin-coated films. Imidization was confirmed by the appearance of the characteristic imide bands near 1785 and 1727 cm^{-1} (imide carbonyl stretching modes) and 1376 cm^{-1} (axial C-N-C stretching mode).

High-resolution XPS C(1s) spectra obtained after imidization of this thin film are shown in Figure 25. The component located at about 288.6 eV (4.0 eV shift from the main component) was characteristic of imide carbonyl groups. The component assigned to the aromatic carbons in PMDA moieties was superimposed upon the component assigned to C-N bonds near 285.6 eV (1.0 eV shift) due to the electron withdrawing effect of the imide carbonyls. However, the relative peak area for these two components was smaller than for fully imidized PMDA/ODA polyimide [51]. Furthermore, a component was observed at 3.2 eV shift from the main carbon peak and was assigned to carboxylate species, supporting the conclusions drawn from the RAIR analysis that formation of polyimide near the oxide surface was at least partially inhibited.

Analysis of thicker films using RAIR and XPS provided additional information showing that the inhibition of imidization was restricted to the near interfacial regions. Figure 26 shows RAIR spectra obtained from a vapor deposited PMDA/ODA film with a thickness of several hundred nanometers as-deposited and after thermal imidization. The spectrum of the as-deposited film (see Figure 26A) was characterized by bands near 1850 and 1780 cm^{-1} due to the symmetric and asymmetric stretching modes of the anhydride C=O, indicating the presence of the PMDA monomer. However, bands were observed near 1663 and 1723 cm^{-1} and attributed to amide and acid groups, respectively, indicating that some polyamic acid formation occurred. After heating, the RAIR spectrum was dominated by strong bands characteristic of polyimides, including those near 1780, 1730 and 1376 cm^{-1} (see Figure 26B). The spectrum after heating was essentially identical to the transmission spectrum of PMDA/ODA polyimide, indicating that the thick vapor deposited films were highly imidized.

The high-resolution XPS C(1s) spectrum obtained after imidization of the thick film is shown in Figure 27. Components due to the imide carbonyl (4.0 eV shift) and the C-N and imide ring carbon (1.1 eV shift) were similar in intensity to those of a fully imidized bulk PMDA/ODA polyimide [51]. These results corroborated the RAIR results and indicated that the films were

highly imidized and that the partially imidized material was restricted to the regions near the oxide surface.

3. Spin-coated PMDA/ODA polyimide on silanated aluminum

Silanation of the aluminum substrates was accomplished by dipping polished, plasma cleaned samples into a 1% solution of γ-aminopropyltriethoxysilane (γ-APS) in water for 10 seconds. The surface was then blown dry using nitrogen and heated under vacuum at 85°C for 10 minutes to remove moisture and condense the silanols into a polysiloxane film. Ellipsometry showed the resulting films were approximately 85 Å thick. Figure 28A shows the RAIR spectrum obtained from a silanated aluminum surface. Broad, weak bands near 1600 and 1500 cm^{-1} were due to the asymmetric and symmetric deformation modes of amino groups protonated with atmospheric CO_2 to form ammonium carboxylate salts [27]. The band near 1080 cm^{-1} was assigned to the Si-O-Si asymmetric stretching mode. The low frequency and broad nature of this band indicated that γ-APS deposited as low molecular weight oligomers, perhaps including some Si-O-Al bonds [27].

PMDA/ODA polyamic acid was spin-coated onto the silanated aluminum from a 0.2% solution in NMP and heated at 100°C to drive off the solvent. RAIR spectra obtained from this film (see Figure 28B) showed bands near 1500 and 1240 cm^{-1} which were assigned to the ODA phenyl ring mode and COC stretching mode, respectively. The broad band near 1650 cm^{-1} was indicative of amide groups. The broad feature near 1610 cm^{-1} was significantly more intense than the phenyl ring mode near 1500 cm^{-1}, especially when compared to spin coated films of similar thickness (c.f., Figure 21). This suggested that additional ammonium carboxylate was formed in the PAA through reaction of carboxylic acid groups with the amino groups of the silane. This was supported by the weak intensity of the band near 1724 cm^{-1} (C=O stretching mode of acid groups), indicating that most acid groups had reacted.

When this film was thermally imidized by heating at 200°C for 1 hour in nitrogen (Figure 28C), new bands characteristic of imide groups appeared near 1785, 1727, and 1376 cm^{-1}. Bands near 1785 and 1727 cm^{-1} were assigned to the asymmetric and symmetric imide C=O stretching modes, respectively. A band attributed to the axial C-N-C stretching mode of imide appeared near 1376 cm^{-1}. Bands attributed to the carboxylate salt were weak or absent after thermal treatment, indicating that imidization was quite complete.

These results showed that γ-APS adsorbed onto aluminum as low molecular weight oligomers which condensed upon heating to form higher molecular weight polysiloxanes. This silane film prevented the formation of the carboxylate salts which were seen when PAA was deposited directly onto an aluminum oxide surface. Instead, acid groups of PAA reacted with amino groups of the silane film to form ammonium carboxylate salts which converted to the corresponding imide upon heating.

F. Fracture energy measurements

1. Circular blister tests of polyimide films on aluminum substrates

The circular blister test was used at UC to measure the adhesive fracture energies of polyimide films deposited onto aluminum substrates. A typical plot of blister pressure P, versus blister height y is shown in Figure 29 for a PMDA/ODA polyimide film that was vapor-deposited

onto an aluminum substrate and then overlaid with a spin-coated film. Pressure versus blister radius a is shown in Figure 30 for the same experiment. Initially, the blister height y increased with blister pressure P, but within the radius of the original blister. Then, at a critical pressure P_c, debonding started and the pressure fell continuously as the blister grew in radius.

Values of P_c and y_c were obtained from experimental data like that shown in Figure 29. The fracture energy G_a was calculated using the expression $G_a = 0.649 P_c y_c$ (equation 1). Table 1 shows the relationship between average fracture energy and substrate preparation for PMDA/ODA on aluminum.

Sample	Fracture Energy (J/m^2) (from equation 1)
PMDA/ODA spin-coated onto bare aluminum	647
PMDA/ODA vapor-deposited onto bare aluminum and overcoated with spin-coated PMDA/ODA	995
PMDA/ODA spin-coated onto aluminum substrate that was silanated with γ-APS	1298
PMDA/ODA spin-coated onto gold-plated steel	422

Table 1. Interfacial fracture energy measured at University of Cincinnati using circular blister test for polyimide films on aluminum and gold substrates.

All of the polyimide films tested had the same bulk structure and composition. As discussed earlier, however, the structure of the interphase region close to the aluminum surface was a strong function of the manner in which the film was deposited. Table 1 shows that the fracture energy of the polyimide/aluminum laminates also depended strongly on the interphase composition. Furthermore, the fracture energy correlated with the relative degree of imidization in the interphase. It was highest for samples with the most imidized interphase, and lowest for those with the least imidized interphase.

Fracture energies determined using equation 1 were much larger than the surface energy of PMDA/ODA (~ 0.1 J/m^2). These results indicated that energy dissipation due to plastic deformation on a global scale or at the crack tip accounted for most of the fracture energy.

2. Failure analysis of blister test specimens - aluminum substrates

a. Vapor-deposited polyimide film

After blister testing, the failure surfaces were analyzed using RAIR and XPS. The RAIR spectrum of the aluminum failure surface of a specimen that was prepared by first vapor-depositing and then spin-coating PMDA/ODA onto polished aluminum is shown in Figure 31. Strong bands characteristic of imide groups appeared near 1785 and 1723 cm^{-1} (asymmetric and symmetric imide carbonyl stretching) and 1376 cm^{-1} (axial C-N-C stretching). The strong,

broad band near 1650 cm^{-1} indicated that there was significant carboxylate salt present on the aluminum surface in addition to polyimide.

Table 2 shows the atomic concentrations of the elements detected on the "aluminum" and "polyimide" failure surfaces. The strong aluminum signal obtained from the aluminum failure surface showed that failure occurred very close to the polymer/metal interface, leaving very little organic material on the oxide surface.

Element	Atomic Concentration (%)	
	Al Surface	PI Surface
Carbon	50	75
Oxygen	33	19
Nitrogen	5	6
Aluminum	13	0.7

Table 2. Composition of substrate and polyimide failure surfaces after circular blister testing of a specimen prepared by first vapor-depositing and then spin-coating PMDA/ODA onto polished aluminum.

The high-resolution C(1s) XPS spectrum obtained from the aluminum failure surface is shown in Figure 32. The component attributed to the imide carbonyls was weaker than for a fully imidized PMDA/ODA polyimide [51]. Also, a component shifted 3.3 eV from the main carbon peak (1.2% of the total peak area) confirmed the presence of carboxylate species. The polyimide present on the aluminum failure surface was partially imidized and contained significant carboxylate.

High-resolution XPS C(1s) spectra obtained from the corresponding polyimide failure surface are shown in Figure 33. The contribution of the imide carbonyl group (288.6 eV, 4.0 eV shift) was 11.4% of the total, and the combined C-imide and C-N component (285.6 eV, 1.0 eV shift) was 33%. The areas under these two components were close to those of a fully imidized PMDA/ODA polyimide [51], indicating that the polyimide on the polymer failure surface had a higher degree of imidization than the polyimide on the aluminum failure surface. Failure occurred very close to the aluminum surface, between the highly imidized polyimide and a mixture of polyimide and carboxylate salt.

b. Spin-coated polyimide film on polished aluminum

The RAIR spectrum of the aluminum failure surface of a specimen prepared by spin-coating PMDA/ODA onto a polished substrate is shown in Figure 34. Besides the imide bands near 1780, 1725 and 1380 cm^{-1}, a strong, broad band assigned to aluminum carboxylate salt was found near 1610 cm^{-1}. These results were similar to those for the vapor-deposited films, indicating that there was partially imidized polymer on the aluminum failure surface. However, much more carboxylate formation and less imidization of the remaining polymer were found on the aluminum failure surface for spin-coated films.

High-resolution XPS C(1s) spectra obtained from the aluminum failure surface further supported the conclusions drawn from RAIR results (see Figure 35). The component shifted upward from the main carbon peak by 3.3 eV was attributed to carbon in carboxylate groups.

This peak represented 5.8% of the total C(1s) peak area, approximately five times more than for the aluminum failure surfaces of vapor-deposited films (1.2%).

The high-resolution XPS C(1s) spectrum obtained from the polyimide failure surface is shown in Figure 36. The presence of a strong imide carbonyl component near 288.6 eV (4.0 eV shift) and the lack of any carboxylate contribution near 287.6 eV (3.0 eV shift) indicated that the polyimide on the polymer failure surface had a higher degree of imidization than that remaining on the aluminum failure surface. These results also indicated that the failure mode was similar to that for vapor deposited films in which the failure occurred between the highly imidized bulk polyimide and an incompletely imidized interphase containing a mixture of polyimide and carboxylate salt.

c. Spin-coated polyimide film on silanated aluminum

The high-resolution C(1s) XPS spectrum obtained from the aluminum failure surface of a blister test specimen prepared by spin-coating PMDA/ODA onto an aluminum substrate that was silanated with γ-APS is shown in Figure 37. The component shifted upward about 4.0 eV from the main carbon peak was characteristic of imide carbonyl groups and was relatively intense, indicating that films left on the aluminum surface were highly imidized. The area of the main carbon peak was 44.8%, which was higher than that of a fully imidized PMDA/ODA polyimide [51]. The excess hydrocarbon may represent the contribution of the silane film.

The high-resolution XPS C(1s) spectrum obtained from the corresponding polymer failure surface is shown in Figure 38. The component near 288.6 eV (4.0 eV shift), which was assigned to the imide carbonyl group, represented 13.9% of the total area under the C(1s) peak. The component near 285.6 eV (1.0 eV shift) was assigned to C-imide and C-N and represented 33.2% of the total area. The areas under these two components were similar to those of a fully imidized PMDA/ODA polyimide [51], indicating that the polymer failure surface was also highly imidized. Failure of adhesion test specimens prepared from silanated substrates appears to have occurred in a zone that included highly imidized polymer.

XPS and IR analysis of the failure surfaces was performed using instruments which obtain signal over a relatively large area of the sample, at least 50 mm^2. However, a few analyses were done using a newly acquired IR microscope with grazing angle objective which allowed RAIR spectra to be obtained from circular areas approximately 25 μm in diameter. Figure 39 shows RAIR spectra obtained from several randomly chosen spots on the aluminum failure surface. It is interesting to note that the spectra obtained from several of these spots were essentially featureless with the exception of a broad doublet with peaks near 1205 and 1170 cm^{-1}. These are significantly higher in frequency than the peaks due to Si-O-Si vibrations seen in the silane films, and their origin is unclear. Only one spot produced a spectrum with bands characteristic of polyimide (spot 2). This spectrum showed no evidence of the Si-O-Si mode near 1100 cm^{-1}, but it did have a peak near 1667 cm^{-1} which was perhaps characteristic of the amides as seen in thin films spin coated onto silanated aluminum surfaces. This spectrum appears to have been obtained from a spot which included well-cured polyimide left on the surface after delamination.

In previous work on SiO_2 surfaces using 90° peel tests, Buchwalter et al. [52] and Anderson et al. [53] reported that silanation of the substrate provided a factor of two increase in

peel strength. Regardless of whether or not the surfaces were silanated, however, the failure locus remained in the bulk polyimide away from the interface. These results were explained by a change in mechanical properties of the polyimide in the near interfacial regions due to interaction with the silane. High temperature curing of the polyimide films results in molecular ordering and a decrease in chain entanglement. When the substrate is silanated, the covalent bonds formed between the polyamic acid and silanated surface at low temperature inhibits this ordering near the interface. The increased entanglement that results provides a stronger polymer in the near-interfacial regions and higher peel strength [7].

In the current study, the analysis tools which sample a relatively large area also suggested that failure occurred completely within the organic phase.. The preliminary microscopic analysis of the failure surfaces, however, suggested that the failure locus may not be homogenous. This could have significant implications for the previously reported results [7,52, 53].

The inhomogenous nature of the failure surfaces suggested that the interface between the silanated aluminum and the polyimide is not optimized. Even though these were the strongest samples evaluated, increasing the amount of amide formation between the aminosilane and the polyamic acid could potentially move the failure more uniformly into the polyimide and increase the fracture energy.

In this study of adhesion between PMDA/ODA polyimide and aluminum, it was shown that interfacial structure correlated well with the adhesion strength. The adhesion strength between polyimide and aluminum substrate was improved by pre-treating the substrates with silane films. These interfaces showed the least amount of carboxylate formation. Vapor-deposited polyimide films had an intermediate value of fracture energy and had significant carboxylate formation at the interface. Spin-coated films on unsilanated aluminum substrates had the greatest amount of carboxylate formation and the lowest interfacial fracture energies. When carboxylate was present, failure typically occurred between the carboxylate containing layer and the well-imidized bulk of the polyimide film.

Carboxylate formation was observed in most cases of polyimide to aluminum adhesion. Its role in the adhesion of polyimide to aluminum is critical. Carboxylate salt was formed through several reactions, including reaction between acid groups of polyamic acid and aluminum hydroxide, reaction between anhydride groups of PMDA and aluminum hydroxide, and reaction between polyamic acid and the primary amines of γ-APS.

The carboxylate salt adhered well to the aluminum surface. Thus, there were always carboxylate species left on aluminum substrates after blister testing for spin-coated and vapor-deposited films. However, formation of carboxylate salt also inevitably led to the partial imidization of polyimide films at the interfacial region, which in turn, caused the formation of a thin layer with inferior mechanical strength and physical properties compared to those highly imidized polyimide. This thin layer, composed of carboxylate and partially imidized polyimide, acted as a weak boundary, leading to fracture between polymer and aluminum. More carboxylate was formed for polyimide spin-coated on bare aluminum than for vapor deposited polyimide, further deteriorating the mechanical strength of the interfacial layer, finally resulting lower fracture energy of adhesion.

In the case of silanated aluminum, the adhesion mechanism was different. When γ-APS adsorbed onto aluminum, it formed low molecular weight oligomers and, perhaps, SiOAl bonds with aluminum. Silane films prevented the reaction between polyamic acid and aluminum to form aluminum carboxylate salts. Instead, acid groups of PAA reacted with amino groups of the silane to form primary bonds and these films could be highly imidized. Silane coupling agents formed primary bonds to both aluminum and polyimide, yielding the highest fracture energy. Also the formation of a weak boundary layer containing carboxylates was eliminated. This, in turn, lead to a much higher fracture energy.

3. Circular blister tests of polyimide films on gold substrates

Previous studies showed that when the polyamic acid of PMDA/ODA was spin-coated onto a gold substrate and then heated, highly imidized films could be obtained with only trace amounts of carboxylate formation [54]. It was expected that the fracture energy required to delaminate a PMDA/ODA film from gold would be much less than that required to delaminate a similar film from an aluminum substrate. That is exactly what was observed (see Table 1). When the blister test was applied to spin-coated polyimide films on gold-plated steel substrates, the average fracture energy was 422 j/m^2.

4. Failure analysis of blister test specimens - gold substrates

After blister testing, the failure surfaces were again analyzed using RAIR and XPS. The RAIR spectrum of the gold failure surface is shown in Figure 40. Bands characteristic of imide groups, which usually appear near 1785, 1723 and 1376 cm^{-1}, were missing. The band near 1240 cm^{-1} characteristic of ODA moieties was not observed either. However, a weak, broad band centered near 1600 cm^{-1} was observed. It was clear that no imide species remained on the gold surface. The band near 1600 cm^{-1} was probably related to a degradation product. Ishida et al. [44] investigated copper-catalyzed degradation of PMDA/ODA polyimide films on copper and found a broad band centered at 1600 cm^{-1}. They assigned this band to a degradation product. However, the copper carboxylate formation could not be ruled out since it appeared in the same region and could not be differentiated. Similarly, the band observed on the gold failure surface was attributed to a degradation product, probably a carboxylate salt.

XPS was used to study both the gold and polymer failure surfaces after blister testing. Strong peaks characteristic of gold were observed in the XPS survey spectra obtained from gold failure surfaces. The atomic concentration of gold on the failure surface was 4.8, 11.0, and 18.1% at take-off angles of 15, 45, and 75 degrees. Carbon and nitrogen concentrations decreased as the take-off angle increased. The concentration of carbon was 80.6, 75.0, and 70.7% at 15, 45, and 75 degrees, respectively. For nitrogen, the concentration was 3.1, 2.8, and 2.1% at 15, 45, and 75 degrees, respectively. The atomic concentrations indicated that failure occurred in the interfacial region since more gold and less organic material were observed as the take-off angle increased.

High-resolution XPS C(1s) spectra obtained from the gold fracture surface are shown in Figure 41. Three components were resolved in this spectrum but none of them was related to imide moieties. The component near 284.6 eV was assigned to hydrocarbon species. A component shifted toward higher binding energies by about 1.6 eV was assigned to carbon singly bonded to oxygen. The third component, shifted about 3.1 eV toward higher binding energy,

was attributed to carbonyl carbons. These results again indicated that degradation products remained on the gold surface. N(1s) spectra further supported this conclusion. One component located near 399.5 eV was found in the N(1s) spectra. This binding energy was lower than expected for an imide nitrogen (400.6 eV) and was probably characteristic of degradation products. RAIR and XPS results obtained from gold failure surfaces indicated that degradation products but no imide species were present on the gold surfaces.

In contrast, atomic concentrations obtained from the polymer failure surface were 71% carbon, 23% oxygen, and 6% nitrogen. These values were close to those expected for a fully imidized bulk polyimide [51]. Little variation as a function of take-off angle was observed. High-resolution XPS C(1s) spectra indicated that polymer failure surface was imidized (see Figure 42). The component due to the imide carbonyl group near 288.5 eV (3.9 eV shift) represented 11.9% of the total area under the C(1s) peak while the component due to C-imide and C-N near 285.6 eV (1.0 eV shift) represented 28.3% of the area. The main component in the N(1s) spectrum was near 400.5 eV, close to the position expected for imide nitrogen (400.6 eV).

Surface analysis of thin polyimide films imidized against gold substrates and failure surface analysis after blister testing showed that there was limited primary bonding between polyimide and gold. Only trace amounts of carboxylate salt formed between polyimide and gold. Secondary bonds, such as Van der Waal's forces, were dominant in adhesion between polyimide and gold and resulted in considerably lower fracture energies than for polyimide/aluminum bonds. The locus of failure was at the polyimide/gold interface, with no imide groups remaining on the gold surface.

G. Finite element analysis [55]

As indicated above, fracture energies determined from blister tests and equation 1 were dominated by energy dissipation due to plastic deformation. Therefore, additional blister tests were conducted at the University of Texas (UT) using specimens prepared at UC. The results were analyzed in two different ways. In one case, equation 1 was used to extract values of the fracture energy assuming elastic deformation. In the other case, finite element analysis was used to determine the effect of global plastic deformation on the fracture energy. Once again, three types of specimens were investigated, including those prepared by spin-coating PMDA/ODA onto bare aluminum, spin-coating PMDA/ODA onto substrates silanated with γ-APS, and spin-coating PMDA/ODA onto aluminum after vapor-deposition of PMDA/ODA. The blisters were pressurized at constant volumetric flow rate and pressures were measured up to and beyond crack initiation. A number of experiments could be conducted on each specimen.

In order to determine the effects of plastic deformation on the fracture energy, the ABAQUS finite element package was used to analyze the experimental configurations. The polyimide was taken to be a J2 flow theory material with isotropic hardening. It was discretized into four-noded shell elements with non-linear kinematics. The aluminum was assumed to be rigid while the interface was represented by a series of non-linear spring elements. The response of these elements was modeled by a cohesive zone model (CZM) characterized by a mixed-mode traction separation law of the type suggested by Wei and Hutchinson [56]. The area under the traction-separation curve (i.e., fracture energy) and the maximum traction level were selected iteratively by fitting the measured and predicted maximum pressure level, the pressure vs.

volume response during quasi-static debonding, and the crack radius and crack-opening displacement histories.

The fracture energies determined from equation 1 were similar for specimens tested at UC and UT and showed the same trends. Specimens prepared by spin-coating PMDA/ODA onto bare aluminum had the lowest fracture energy while those prepared by spin-coating PMDA/ODA onto substrates silanated with γ-APS had the highest. When PMDA/ODA was vapor-deposited onto aluminum and overcoated with spin-coated PMDA/ODA, the fracture energy was intermediate. Fracture energies measured at UC were generally greater than those measured at UT. This was probably related to differences in the way in which the central deflection of the blister was determined at UC and UT.

It was found that different traction-separation laws were required to represent the behavior of the various specimens (see Table 3). When specimens were prepared by spin-coating PMDA/ODA onto bare aluminum, the fracture energy was low, 579 J/m^2. However, the fracture energy increased to 705 J/m^2 for specimens prepared by vapor-deposition of PMDA/ODA onto bare aluminum followed by spin-coating with PMDA/ODA. The fracture energy was highest, 750 J/m^2, when PMDA/ODA was spin-coated onto aluminum substrates silanated with γ-APS.

Sample	**Fracture Energy (J/m^2) (from equation 1)**	**Fracture Energy (J/m^2) (from cohesive zone model)**
PMDA/ODA spin-coated onto bare aluminum	646	579
PMDA/ODA vapor-deposited onto bare aluminum and overcoated with spin-coated PMDA/ODA	883	705
PMDA/ODA spin-coated onto aluminum substrate that was silanated with γ-APS	901	750

Table 3. Interfacial fracture energies measured at the University of Texas using circular blister test for polyimide films on aluminum substrates.

As shown in Table 3, the fracture energies obtained from the cohesive zone model were less than those extracted using equation 1 and the approach suggested by Gent and Lewandowski [33]. This is because the effects of plasticity in the central displacements were eliminated in the CZM. However, the difference, approximately 15%, was not great and it was concluded that plasticity on a global scale made only a small contribution to the fracture energy in the circular blister test. The fracture energies determined using the CZM model were still much larger than the surface energy of the polymer, which was expected to be no more than 0.1 J/m^2. This indicated that another energy dissipation process, such as crack tip plasticity, was operative.

Although the fracture energies determined using the CZM were greater than the surface energy of the polyimide, they were still less than the fracture energy, which is approximately 1,000 J/m^2 [57]. This reflects the fact that failure in the blister tests was always within an "interphase" that had a different composition than the bulk of the polyimide.

IV. Conclusions

- When polyimides having relatively flexible backbones, such as those from PMDA/4-BDAF and 6FDA/ODA, were spin-coated against aluminum substrates, they formed films in which there was little preferred orientation of the polymer molecules.
- Imidization of spin-coated polyamic acids to polyimides was inhibited by interaction of acid groups with aluminum to form aluminum carboxylate species.
- Langmuir-Blodgett (LB) films of alkylamine salts of the polyamic acid of PMDA/ODA were deposited onto silver substrates mainly as salts which were easily imidized.
- After imidization of LB films, the axis of the PMDA moieties was tilted away from the surface normal by about 70°, showing that the molecular axis of the PMDA/ODA polyimide molecules had a preferred orientation which was nearly parallel to the silver surface.
- 4-Mercaptophenylphthalimide (4-MPP) chemisorbed onto gold through the thiol groups.
- The molecular axis of 4-MPP was tilted from the normal to the gold surface by about 21°.
- PMDA chemisorbed onto aluminum from the vapor to form carboxylate salts.
- ODA physisorbed onto aluminum from the vapor.
- When PMDA and ODA monomers were co-adsorbed onto aluminum substrates from the vapor, the monomers reacted to form polyamic acid.
- When the effects of plastic deformation were ignored, the fracture energy required to delaminate spin-coated PMDA/ODA polyimide films from aluminum substrates was relatively low, ~ 650 J/m^2.
- The fracture energy required to delaminate spin-coated PMDA/ODA films from aluminum substrates increased to about 1298 J/m^2 when the substrates were pre-treated with a dilute aqueous solution of γ-aminopropyltriethoxysilane (γ-APS).
- The fracture energy required to delaminate vapor-deposited PMDA/ODA films from aluminum was about 995 J/m^2.
- The fracture energy required to delaminate spin-coated PMDA/ODA films from gold was relatively low, about 422 J/m^2.
- Finite element analysis showed that energy dissipation due to global plastic deformation of spin-coated PMDA/ODA films during blister tests was less than about 15% of the total fracture energy.
- Even when the effects of global plastic deformation were accounted for, the fracture energy required to delaminate a PMDA/ODA film from aluminum was much greater than the surface energy of the polyimide (~ 0.1 J/m^2).
- An energy dissipation process, such as plasticity at the crack tip, makes a significant contribution to the fracture energy measured by the blister test.

- Carboxylate salt formation was highest for spin-coated films on aluminum and lowest for spin-coated films on silanated aluminum substrates. Vapor-deposited films had an intermediate level of carboxylate formation.
- Formation of carboxylate salts led to the partial imidization of polyimide films in the interfacial region and caused the formation of a thin layer with inferior mechanical strength and physical properties compared to those of highly imidized polyimide.
- This thin layer acted as a weak boundary layer, and was the locus of failure during fracture mechanics experiments.

V. References

1. S.D. Senturia, Polymeric Mat. Sci. Eng. **55**, 385 (1986).
2. A.M. Wilson, Thin Solid Films **83**, 145 (1981).
3. R.J. Jensen, Polymeric Mat. Sci. Eng. **55**, 413 (1986).
4. M.-J. Brekner and C. Feger, J. Poly. Sci. Poly. Chem. **25**, 2005 (1987).
5. C. Feger, Poly. Eng. Sci. **29**, 347 (1989).
6. M.-J. Brekner and C. Feger, J. Poly. Sci. Poly. Chem. **25**, 2479 (1987).
7. L.P. Buchwalter, in Polyimides: Fundamentals and Applications, M.K. Ghosh and K.L. Mittal, eds., Marcel Dekker, NY, 1996, p. 587.
8. J. Kim, S.P. Kowalczyk, Y.H. Kim, N.J. Chou, and T.S. Oh, Mater. Res. Soc. Symp. Proc. **167**, 137 (1990).
9. J.R. Salem, F.O. Sequeda, J. Duran, W.Y. Lee, and R.M. Yang, J. Vac. Sci. Technol. **A4**, 369 (1986).
10. S.P. Kowalczyk, C.D. Dimitrakopoulos, and S.E. Molis, Mater. Res. Soc. Symp. Proc. **227**, 55 (1991).
11. M. Grunze and R.N. Lamb, Chem. Phys. Lett. **133**, 283 (1987).
12. M. Grunze and R.N. Lamb, Surf. Sci. **204**, 183 (1988).
13. R.N. Lamb, J Baxter, M. Grunze, C.W. Kong, and W.N. Unertl, Langmuir **4**, 249 (1988).
14. T. Strunskus, M. Grunze, and S. Gnanarajan, in Metallization of Polymers, ACS Symposium Series no. 440, E.S. Sacher, J.J. Pireaux, and S.P. Kowalczyk, eds., American Chemical Society, 1990.
15. S.S. Perry and A. Campion, Surf. Sci. Lett. **234**, L275 (1990).
16. R.G. Mack, H.H. Patterson, M.R. Cook, and C.M. Carlin, J. Polym. Sci.: Polym. Lett. Ed. **27**, 25 (1989).
17. R.G. Pethe, C.M. Carlin, and H.H. Patterson, J. Mater. Res. **8**, 3218 (1993).
18. M. Kakimoto, M. Suzuki, T. Konishi, Y. Imai, M. Iwamoto, and T. Hino, Chem. Lett. 823 (1986).

19. M. Kakimoto, T. Konishi, A. Morikawa, and Y. Imai, Polymer Journal **20**, 269 (1988).

20. I. Fujiwara, G. Ishimoto, and J. Seto, J. Vac. Sci. Technol. **B9**, 1148 (1991).

21. H. Sotobayashi, T. Schilling, and B. Tesche, Langmuir **6**, 1246 (1990).

22. J.Y. Fang, Z.H. Liu, G.W. Min, and Y. Wei, Liquid Crystals **14**, 1621 (1993).

23. X.M. Yang, N. Gu, Z.H. Liu, and Y. Wei, Phys. Lett. **A183**, 111 (1993).

24. X.M. Yang, G.W. Min, N. Gu, Z.H. Liu, and Y. Wei, J. Vac. Sci. Technol. **B12**, 1981 (1994).

25. L.P. Buchwalter, J Adhesion Sci. Technol. **4**, 9 (1990) 697.

26. H. Linde and R.T. Gleason, J. Polym. Sci. Polym. Chem. Ed. **22** 3043 (1984).

27. F.J. Boerio and C.A. Gosselin, in Advances in Chemistry Series, vol. 203, C.D. Craver, ed., American Chemical Society, Washington, DC, 1983, p. 541.

28. H.D. Goldberg, G.S. Cha, and R.B. Brown, J. Appl. Polym. Sci. **43**, 1287 (1991).

29. T.S. Oh, L.P. Buchwalter, and J. Kim, J. Adhesion Sci. Technol. **4**, 303 (1990).

30. J.L. Goldfarb, R.J. Farris, Z. Chai, and F.E. Karasz, Mater. Res. Soc. Symp. Proc. **227**, 335 (1991).

31. K.-S. Kim and J.-H. Kim, ASME Trans. J. Eng. Mater. Technol. **110**, 206 (1988).

32. K.-S. Kim and N. Aravas, Intl. J. Solids Struct. **24**, 417 (1988).

33. A.N. Gent and L.H. Lewandowski, J. Appl. Polym. Sci. **33**, 1567 (1987).

34. F.L. McCrackin and J. Colson, Nati. Bur. Stds. Tech. Note 242, U. S. Govt. Print. Off., Washington, D. C., 1964.

35. W.W. Zhao, M.S. Thesis, University of Cincinnati, 1995.

36. L.P. Buchwalter and A.I. Baise, in Polyimides: Synthesis, Characterization and Applications, vol. 2, K.L. Mittal, ed., Plenum Press, NY, 1984, p. 537.

37. W. H. Tsai, N. G. Cave, and F. J. Boerio, Langmuir **8**, 927 (1992).

38. W. W. Zhao and F. J. Boerio, Surf. Interf. Anal. **26**, 316 (1998).

39. P.M. Cotts, in Polyimides: Synthesis, Characterization, and Properties, vol. 1, K.L. Mittal, ed., Plenum Press, New York, 1984, p. 223.

40. J.T. Young, W.H. Tsai, and F.J. Boerio, Macromolecules **25**, 887 (1992).

41. J.T. Young, F.J. Boerio, Z. Zhang, and T.L. Beck, Langmuir **12**, 1219 (1996).

42 Z. Zhang, T.L. Beck, J.T. Young, and F.J. Boerio, Langmuir **12**, 1227 (1996).

43. Y.H. Kim, J. Kim, G.F. Walker, C. Feger, and S.P. Kowalczyk, J. Adhesion Sci. Technol. **1**, 331 (1987).

44. K. Kelley, Y. Ishino, and H. Ishida, Thin Solid Films **154**, 271 (1987).

45. D.L. Allara, in Adhesion and Adsorption of Polymers, Part B, L.-H. Lee, ed., Plenum

Press, N.Y., 1980, p. 751.

46. W.H. Tsai, N.G. Cave, and F.J. Boerio, Langmuir **8,** 927 (1992).

47. F.M. Fowkes and M.A. Mostafa, Ind. Eng. Chem. Prod. Res. Dev. **17,** 3 (1978).

48. S.P. Kowalczyk, Y.H. Kim, G.F. Walker, and J. Kim, J. Vac. Sci. Technol. **A6**, 1377 (1988).

49. M. Grunze and R.N. Lamb, Chem. Phys. Lett. **133**, 4 (1987) 233.

50. M. Grunze and R.N. Lamb, Surface Sci. **204**, 183 (1988).

51. J.T. Young, Ph.D. Dissertation, University of Cincinnati, 1994.

52. L.P. Buchwalter and J. Greenblatt, J Adhesion **19,** 257 (1986).

53. H.R. Anderson, Jr., M.M. Khojasteh, T.P. McAndrew, and K.G. Sachdev, IEEE Trans. CHMT **9,** 364 (1986).

54. J.T. Young and F.J. Boerio, Surf. Interf. Anal. **20**, 341 (1993).

55. A. Shirani, K.M. Liechti, S. Weaver, and F. J. Boerio, J. Adhesion, to be submitted, 1998.

56. Y. Wei and J. W. Hutchinson, Division of Engineering and Applied Sciences, Harvard University, Mech. 315 (1996).

57. A. Shirani, Ph.D. Dissertation, University of Texas, 1997.

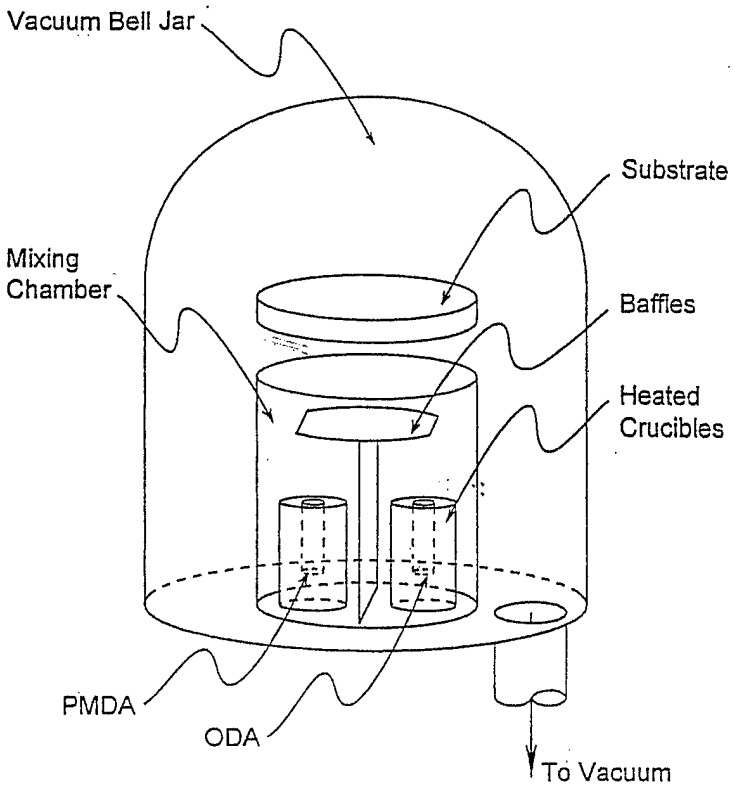

Figure 1. Diagram of apparatus for vapor deposition of PMDA and ODA monomers.

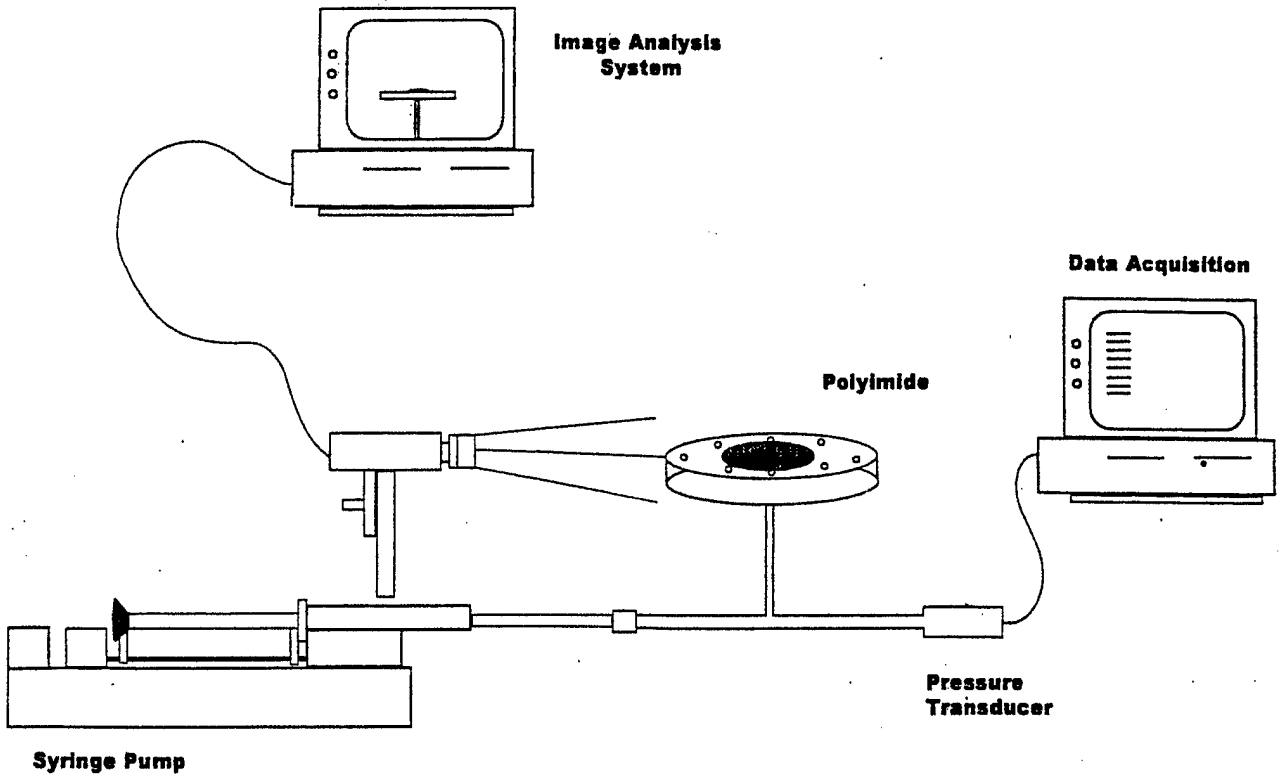

Figure 2. Diagram of blister testing apparatus at the University of Cincinnati (UC).

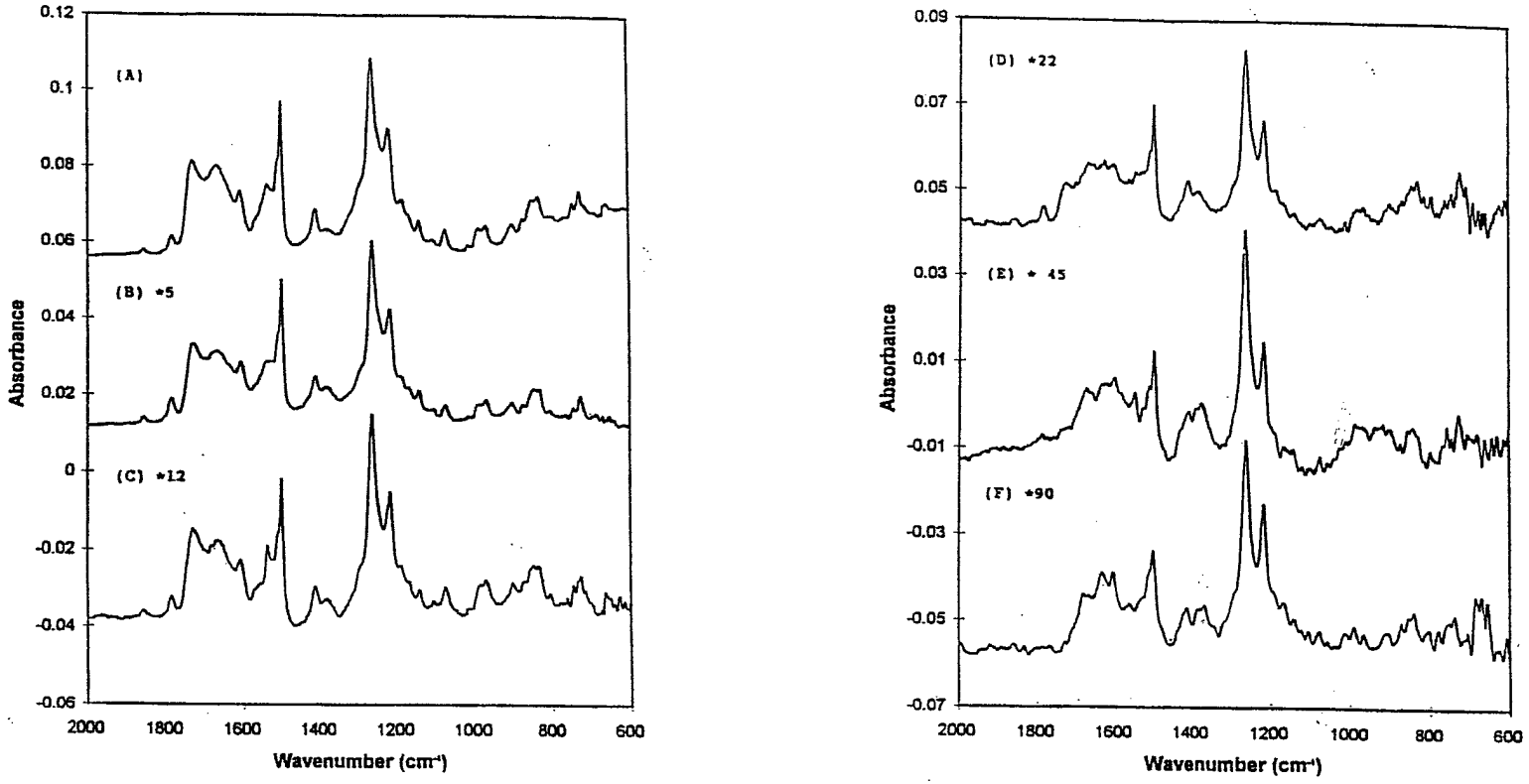

Figure 3. RAIR spectra of films of 6FDA/ODA polyamic acid spin-coated onto aluminum substrates from (A) - 4%, (B) - 1.6%, (C) - 0.8%, (D) - 0.4%, (E) - 0.2% and (F) - 0.1% solutions in N-methylpyrrolidone (NMP).

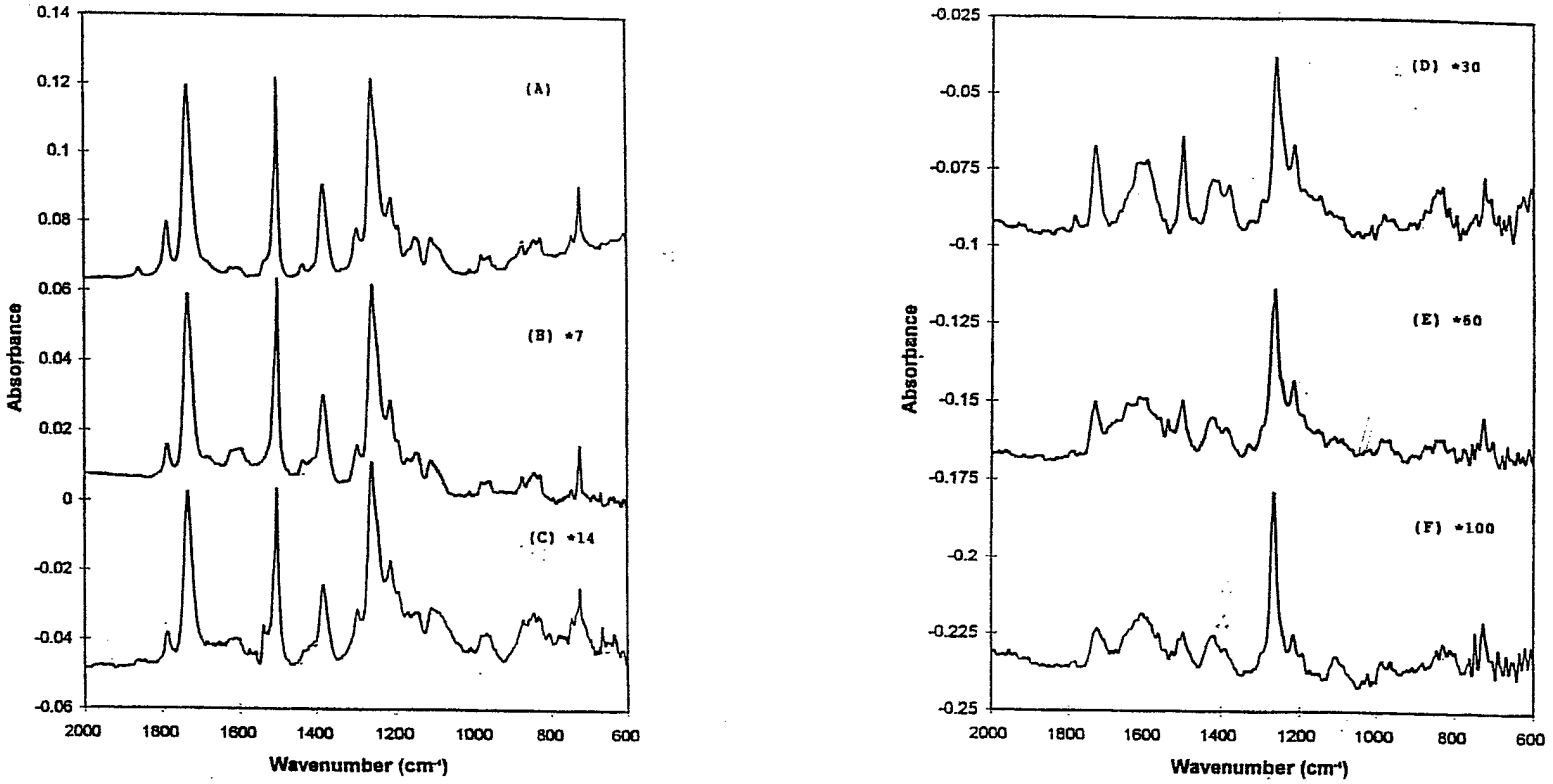

Figure 4. RAIR spectra of films of 6FDA/ODA polyamic acid spin coated onto aluminum substrates from (A) - 4%, (B) - 1.6%, (C) - 0.8%, (D) - 0.4%, (E) - 0.2% and (F) - 0.1% solutions in NMP and imidized.

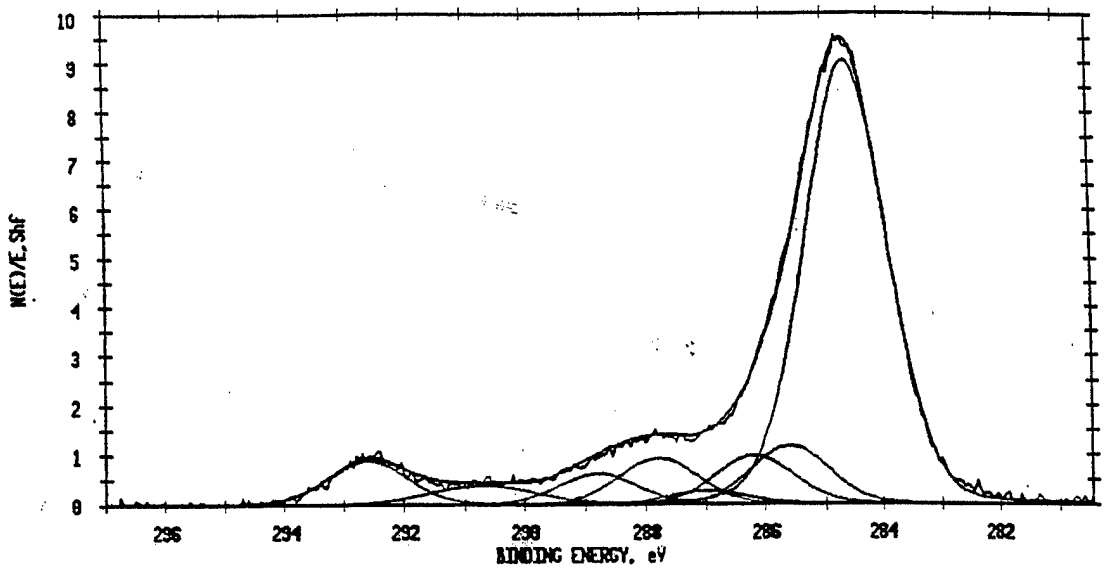

Figure 5. C(1s) XPS spectra obtained from 6FDA/ODA polyamic acid spin-coated onto aluminum from a 0.2% solution in NMP.

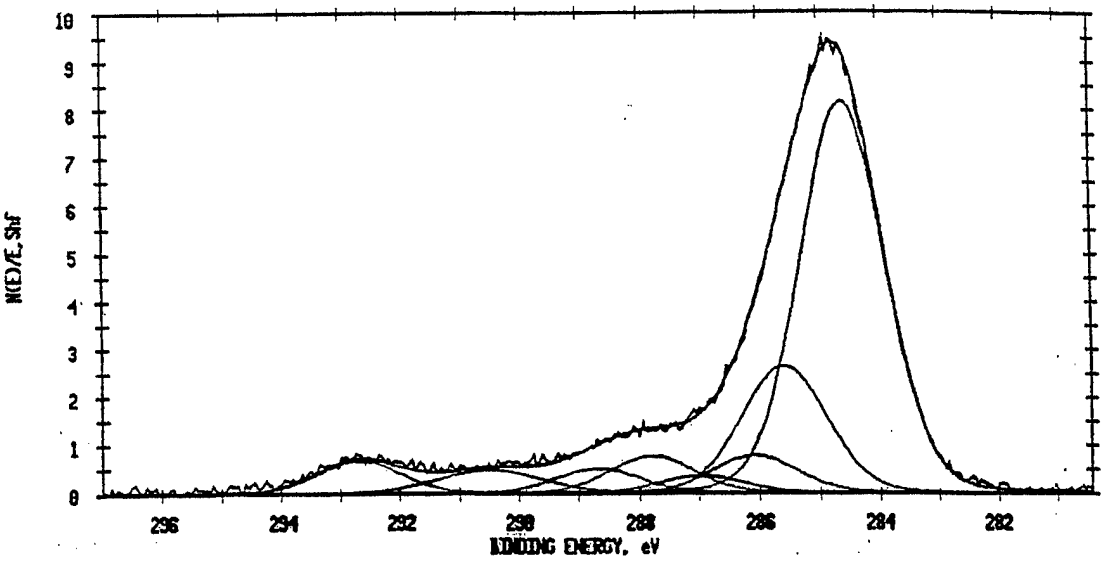

Figure 6. C(1s) XPS spectra obtained from 6FDA/ODA polyamic acid spin-coated onto aluminum from a 0.2% solution in NMP after thermal imidization.

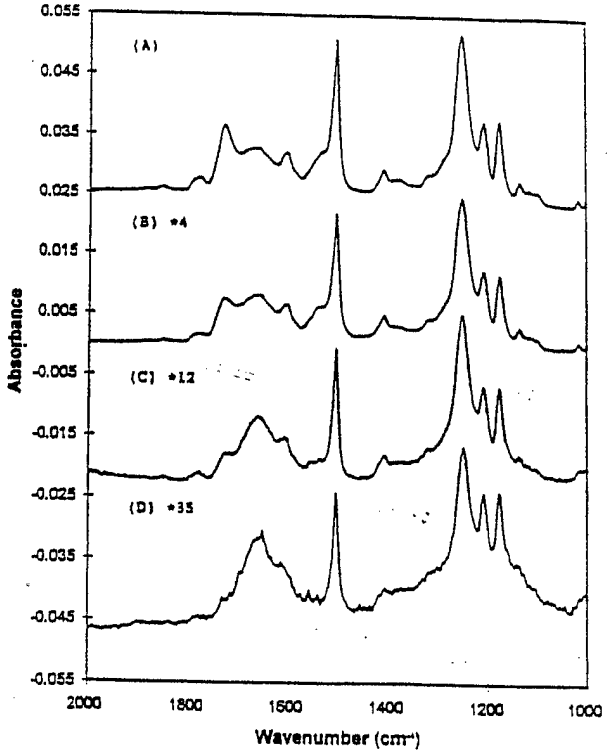

Figure 7. RAIR spectra of films of PMDA/4-BDAF polyamic acid spin-coated onto aluminum from (A) - 2.5%, (B) - 0.8%, (C) - 0.2%, and (D) - 0.1% solutions in N-methylpyrrolidone (NMP).

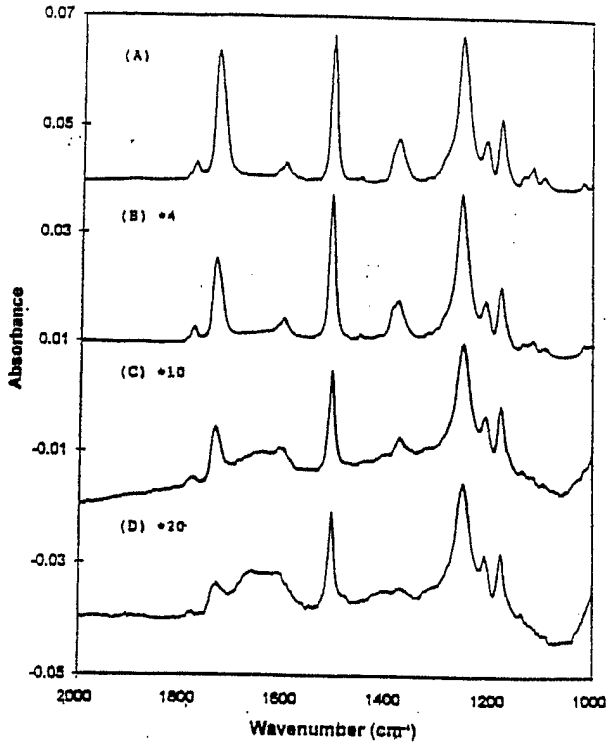

Figure 8. RAIR spectra of films of PMDA/4-BDAF polyamic acid spin-coated onto aluminum from (A) - 2.5%, (B) - 0.8%, (C) - 0.2%, and (D) - 0.1% solutions in NMP and then thermally imidized.

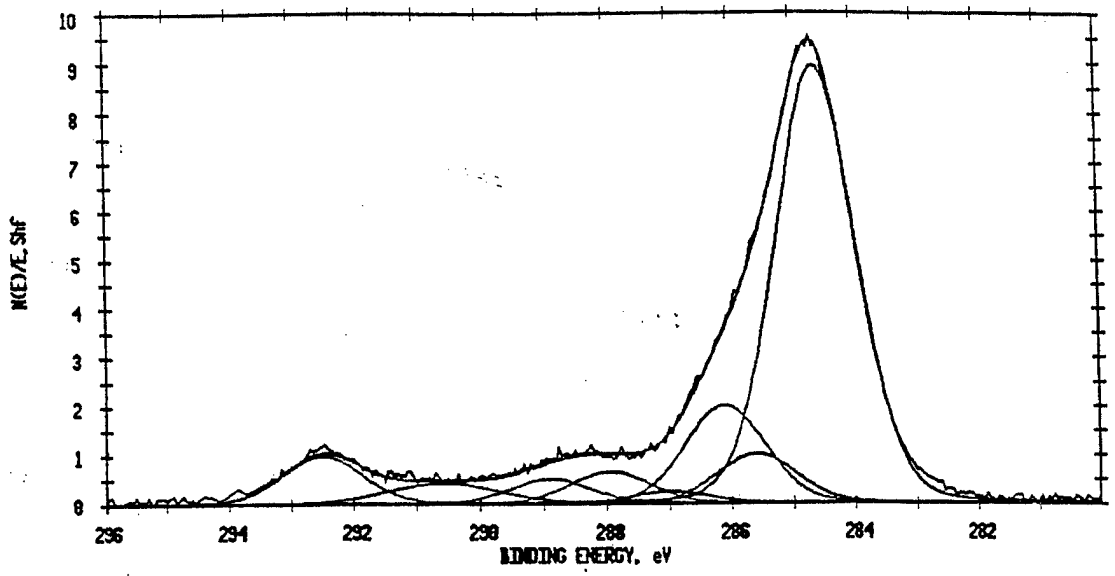

Figure 9. C(1s) XPS spectra obtained from PMDA/4-BDAF polyamic acid spin-coated onto aluminum from 0.2% solution in NMP.

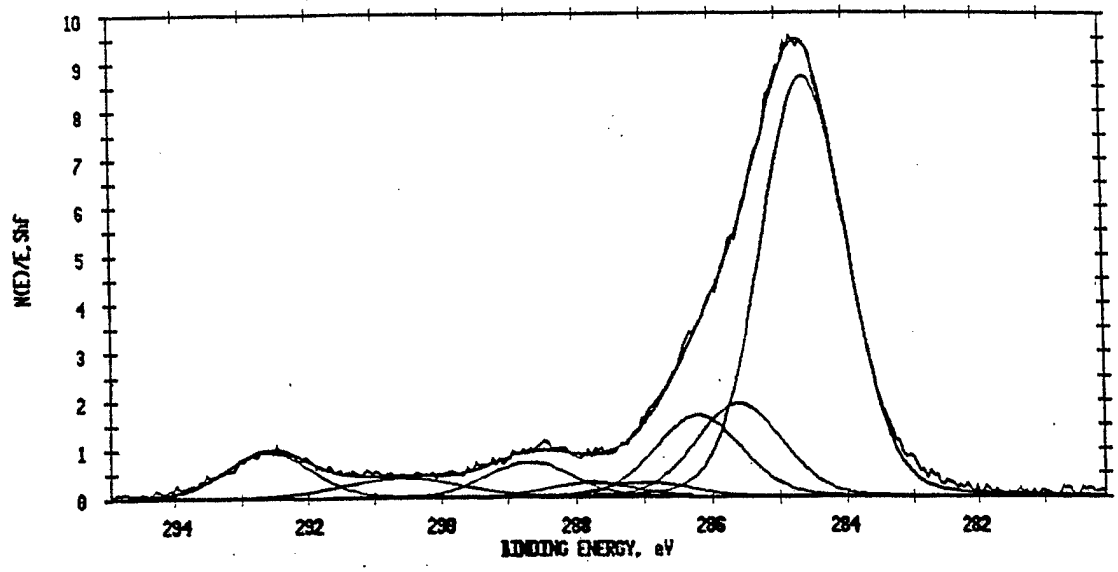

Figure 10. C(1s) XPS spectra obtained from PMDA/4-BDAF polyamic acid spin-coated onto aluminum from 0.2% solution in NMP and then thermally imidized.

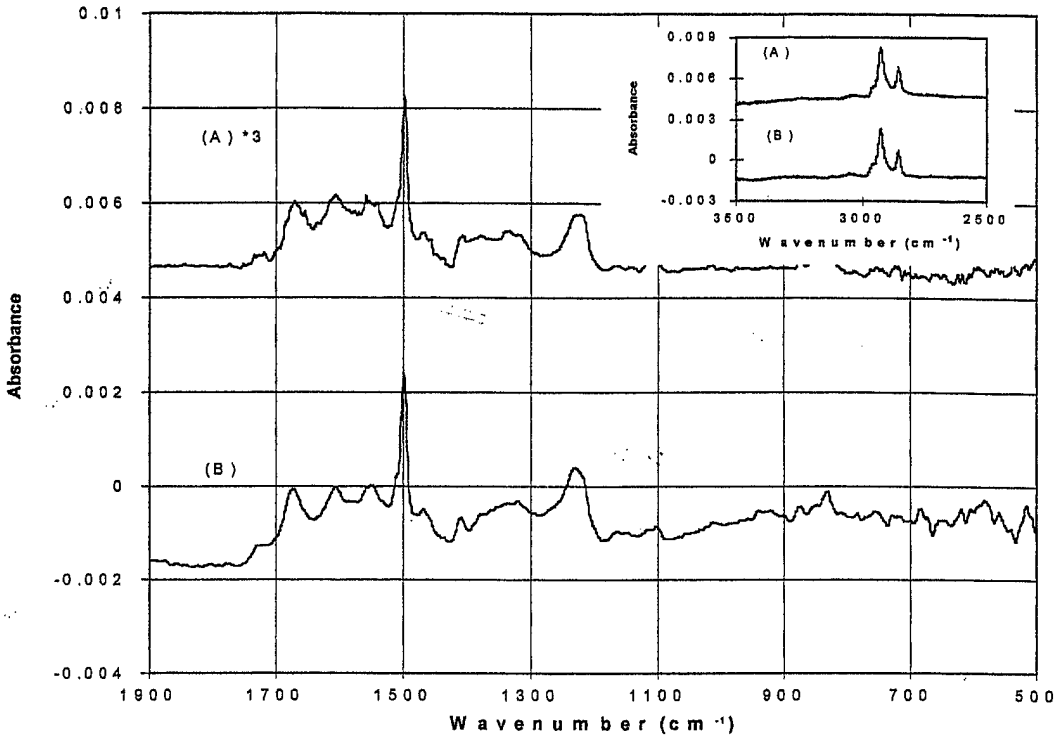

Figure 11. RAIR spectra of (A) - 1-layer and (B) - 3-layer Langmuir-Blodgett films of PMDA/ODA polyamic acid dimethylhexadecylamine salt on silver substrates.

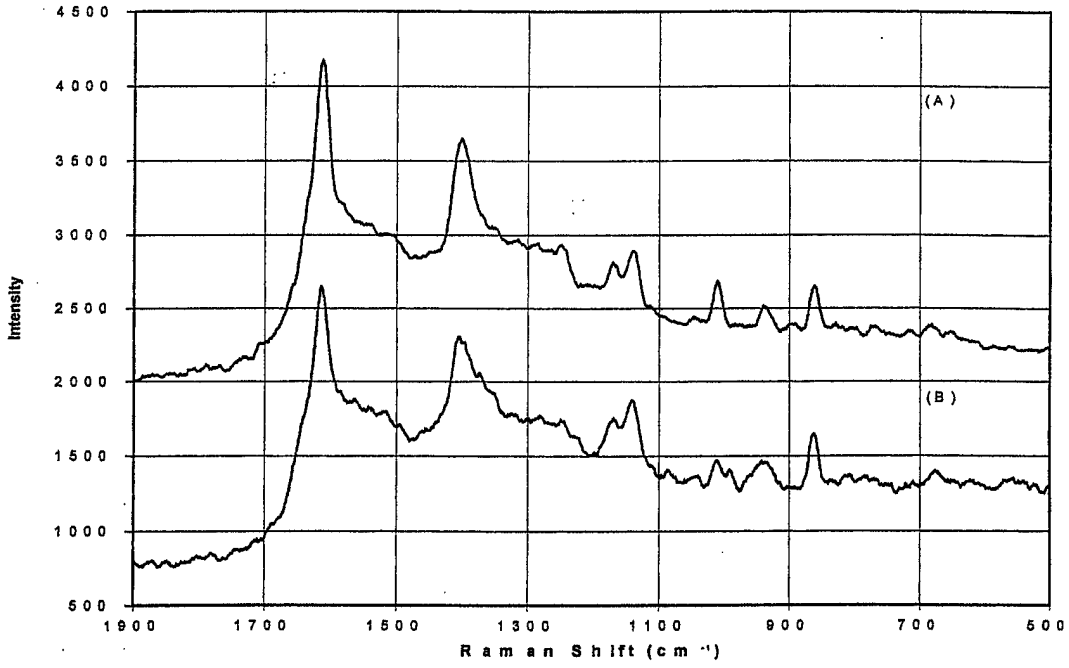

Figure 12. SERS spectra of (A) - 1-layer and (B) - 3-layer Langmuir-Blodgett films of PMDA/ODA polyamic acid dimethylhexadecylamine salt on silver substrates.

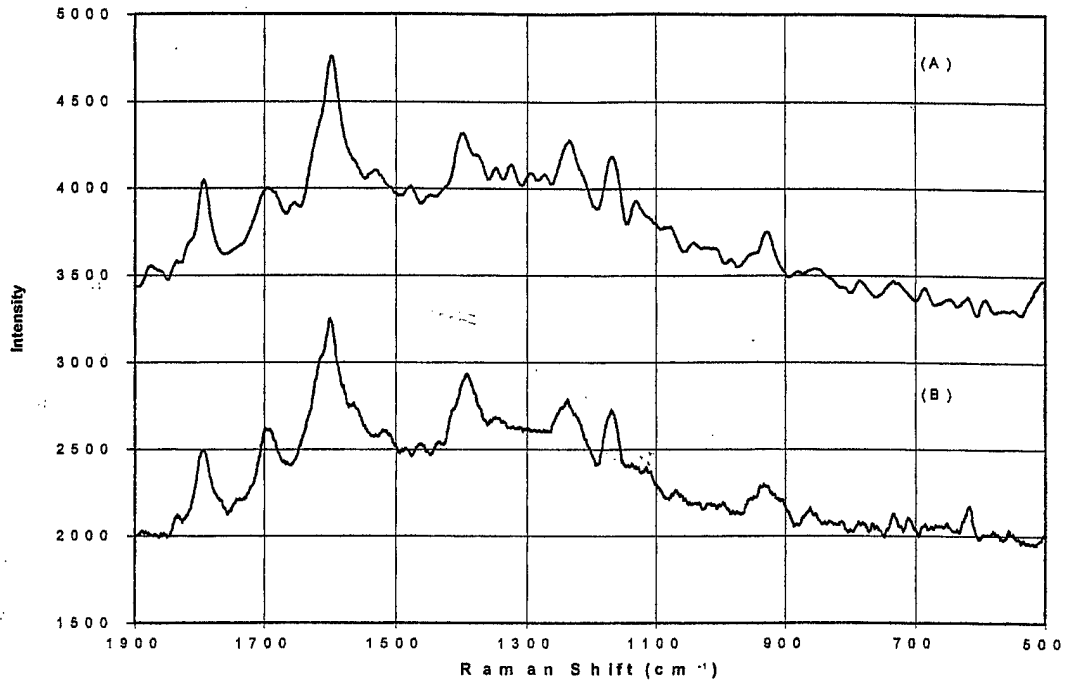

Figure 13. SERS spectra of (A) - 1-layer and (B) - 3-layer Langmuir-Blodgett films of PMDA/ODA polyamic acid dimethylhexadecylamine salt on silver substrates after imidization.

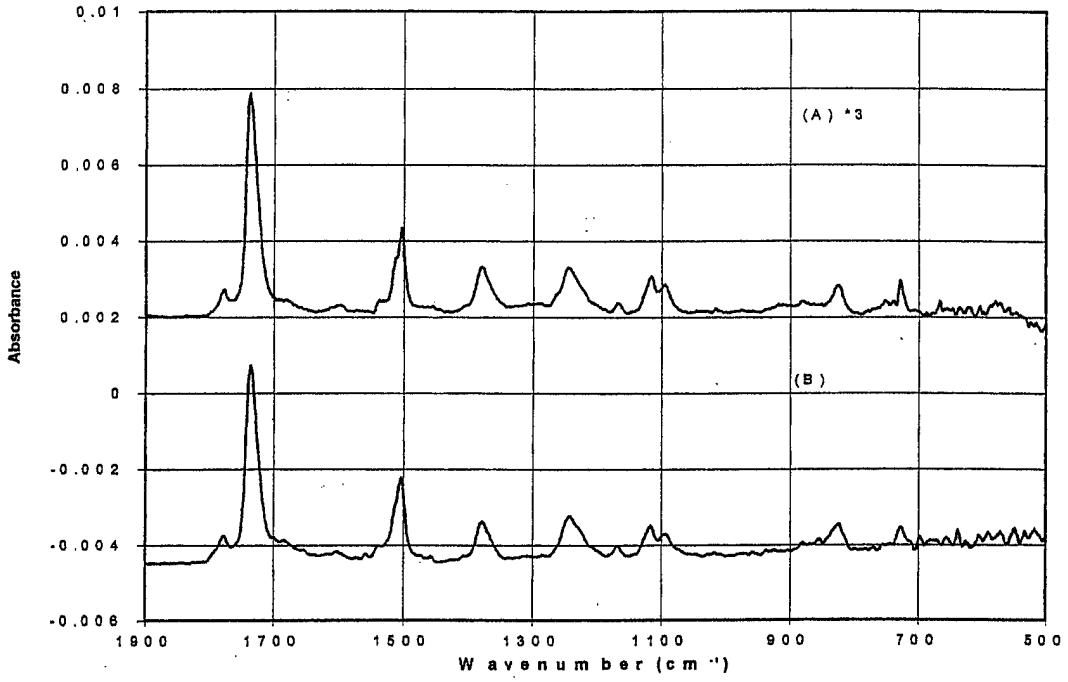

Figure 14. RAIR spectra of (A) - 1-layer and (B) - 3-layer Langmuir-Blodgett films of PMDA/ODA polyamic acid dimethylhexadecylamine salt on silver substrates after imidization.

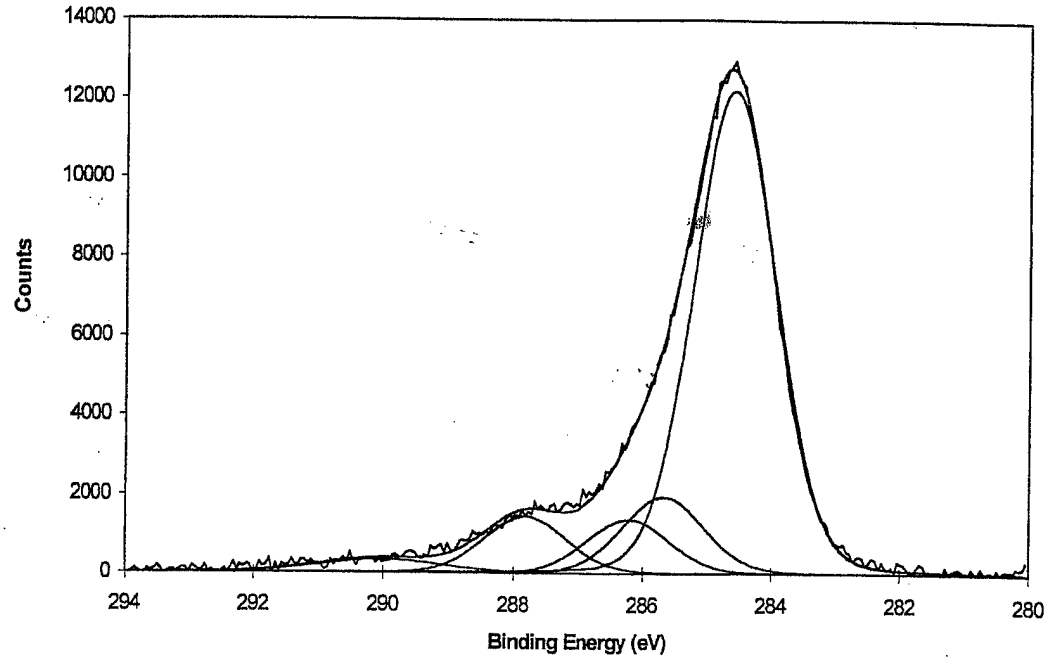

Figure 15. C(1s) XPS spectrum obtained from a 1-layer Langmuir-Blodgett film of PMDA/ODA polyamic acid dimethylhexadecylamine salt on a silver substrate.

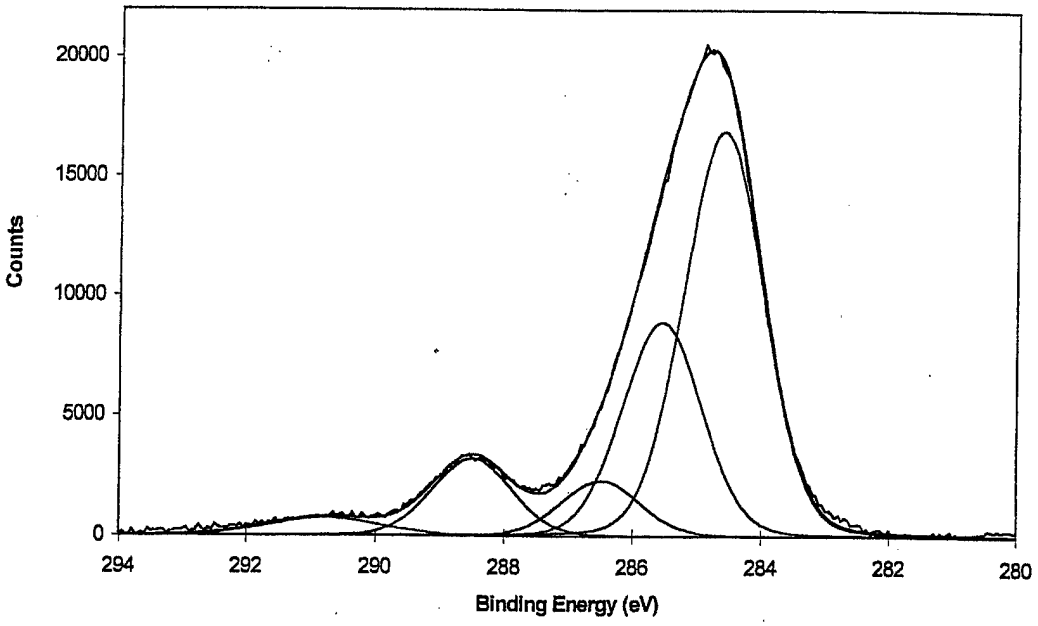

Figure 16. C(1s) XPS spectrum obtained from a 1-layer Langmuir-Blodgett film of PMDA/ODA polyamic acid dimethylhexadecylamine salt on a silver substrate after imidization.

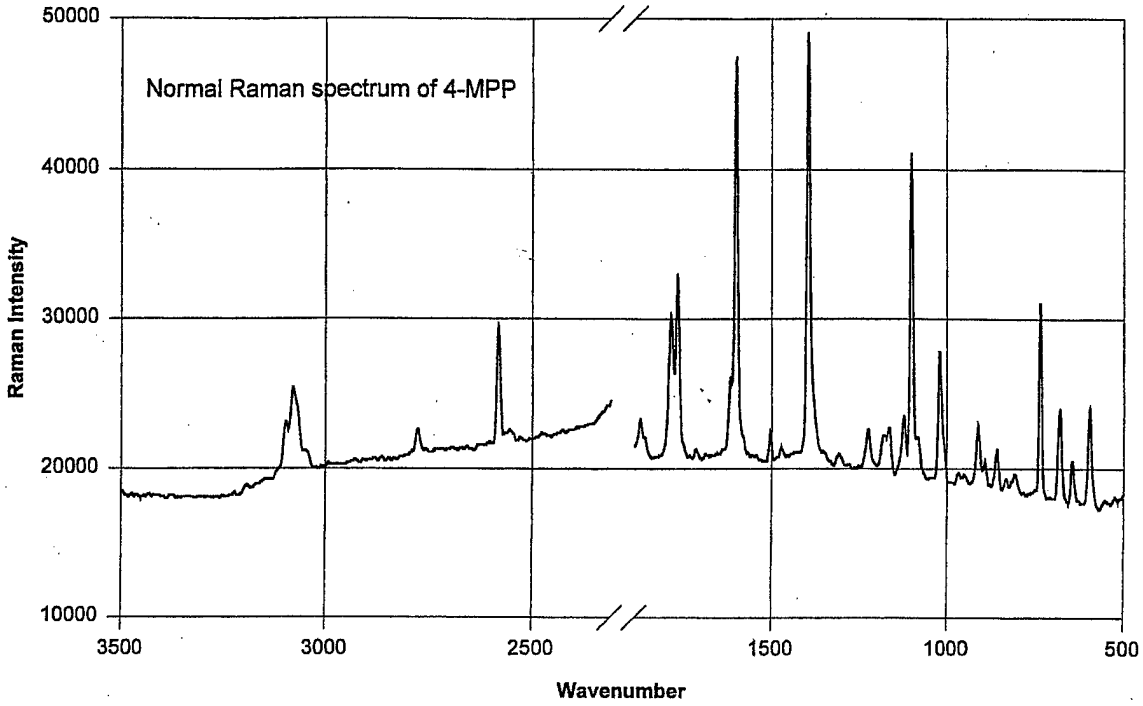

Figure 17. The normal Raman spectrum of neat 4-MPP.

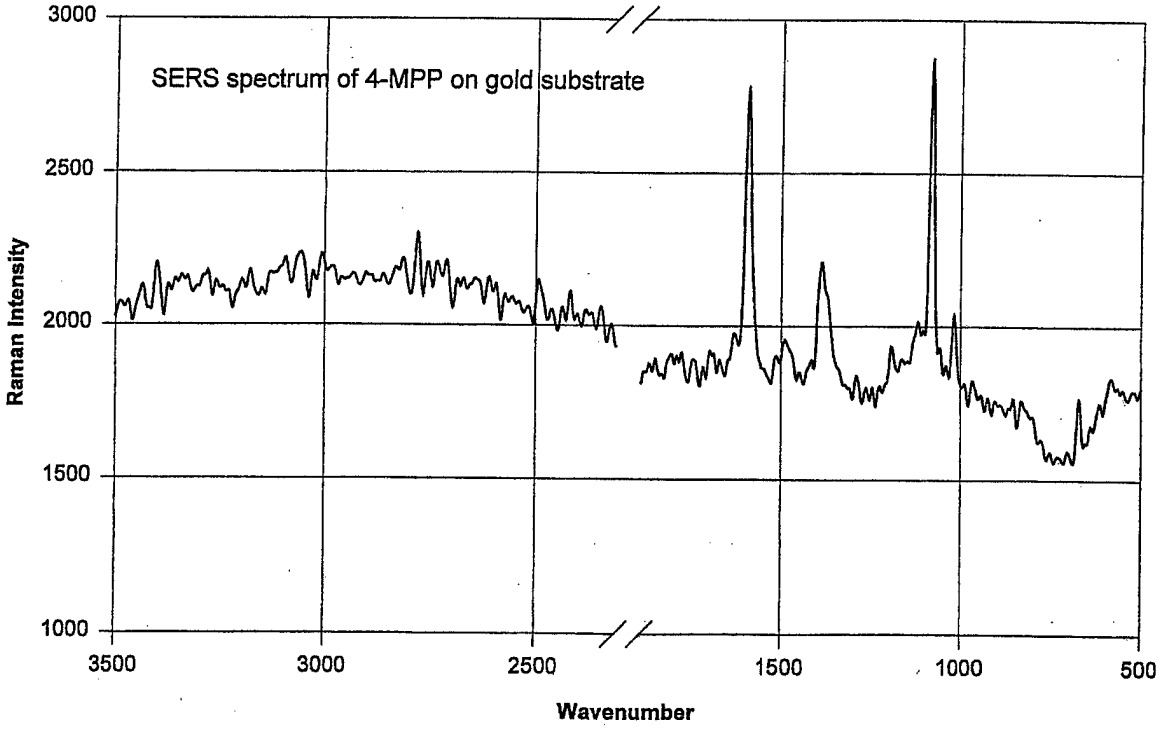

Figure 18. The SERS spectrum of a 4-MPP monolayer on a gold substrate.

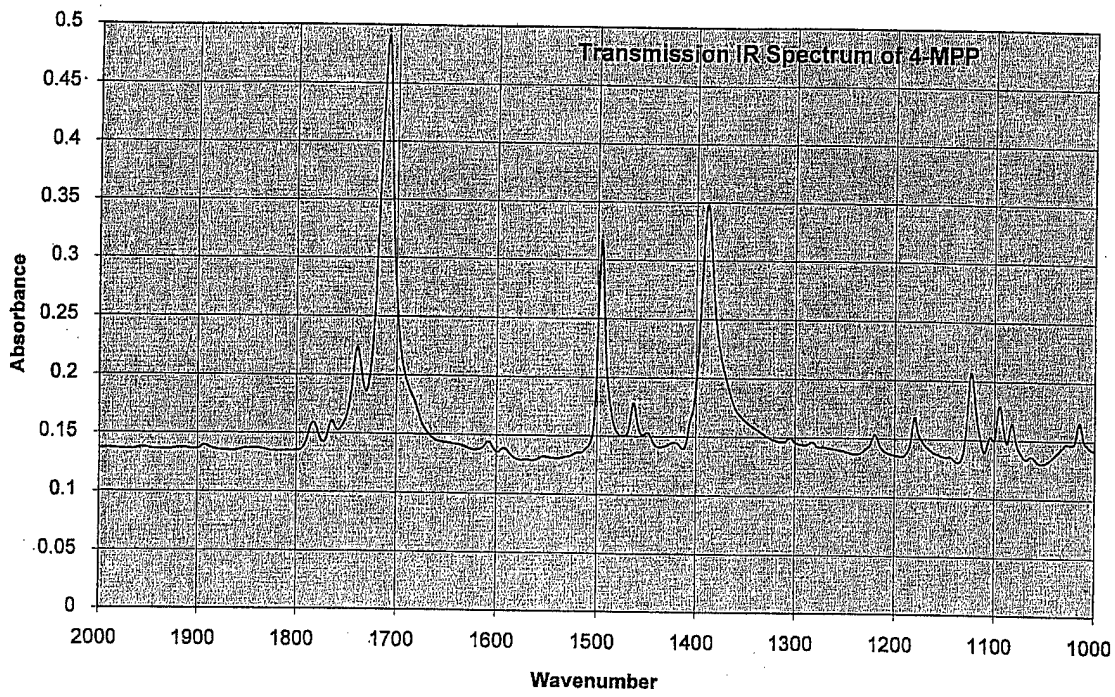

Figure 19. Transmission infrared spectrum of neat 4-MPP.

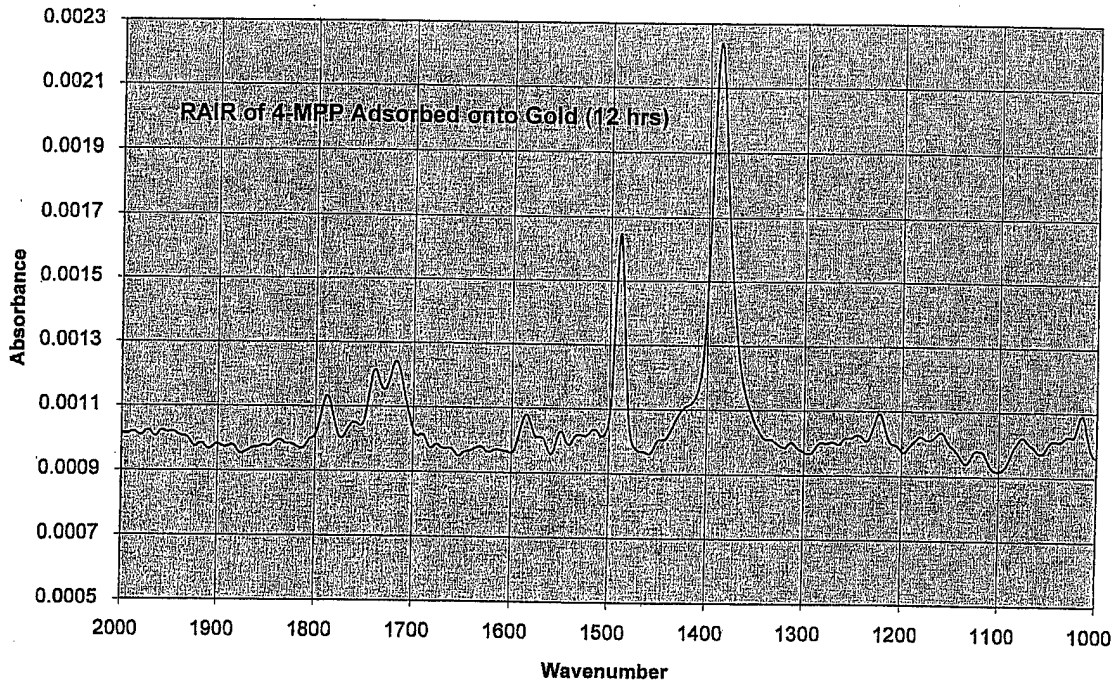

Figure 20. RAIR spectrum of a 4-MPP monolayer on a gold substrate.

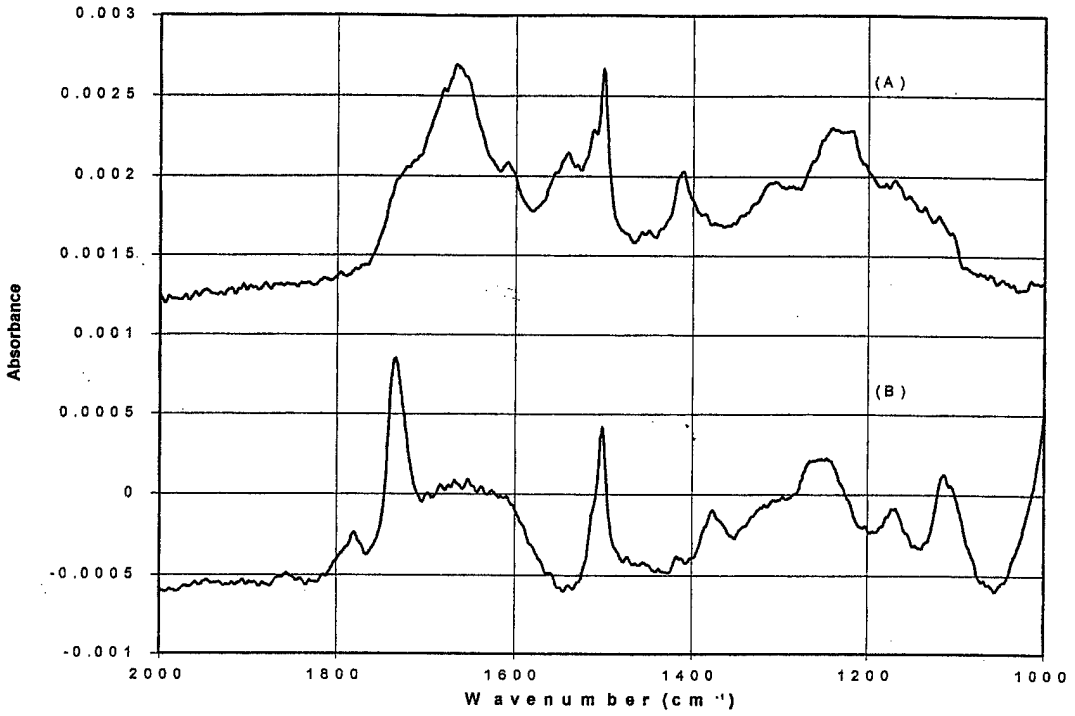

Figure 21. RAIR spectrum of PMDA/ODA polyamic acid spin-coated onto aluminum from 0.2% NMP solution: (A) - heated to 100°C (B) - heated to 200°C.

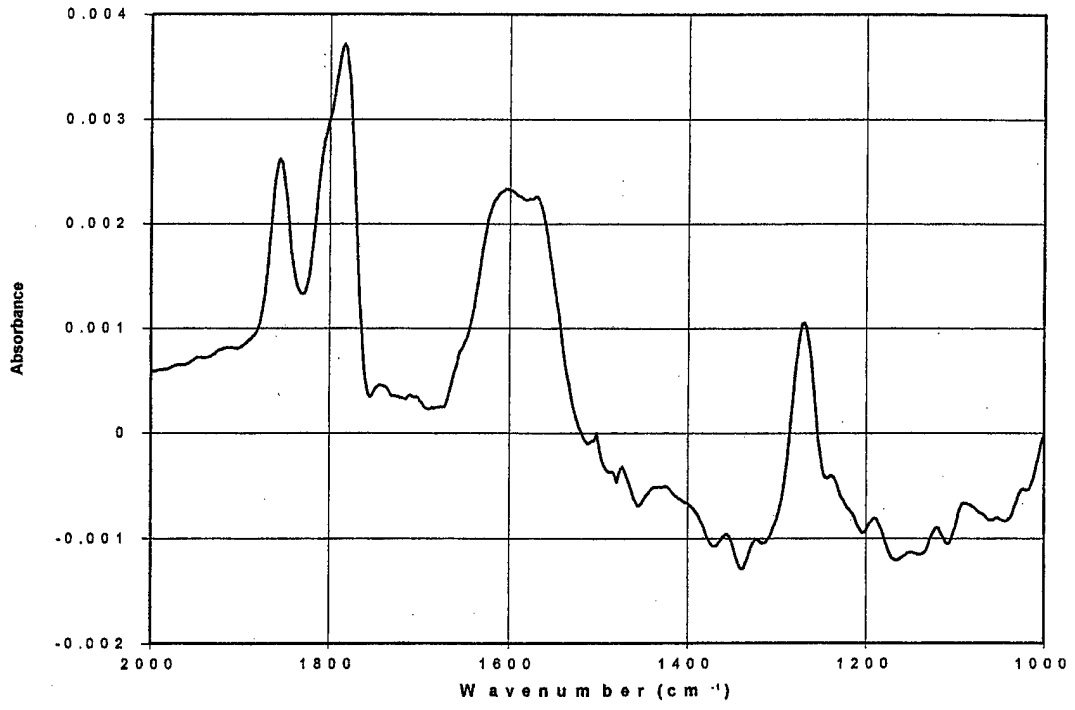

Figure 22. RAIR spectrum of a vapor-deposited PMDA film on an aluminum substrate. The film thickness was approximately 30 Å.

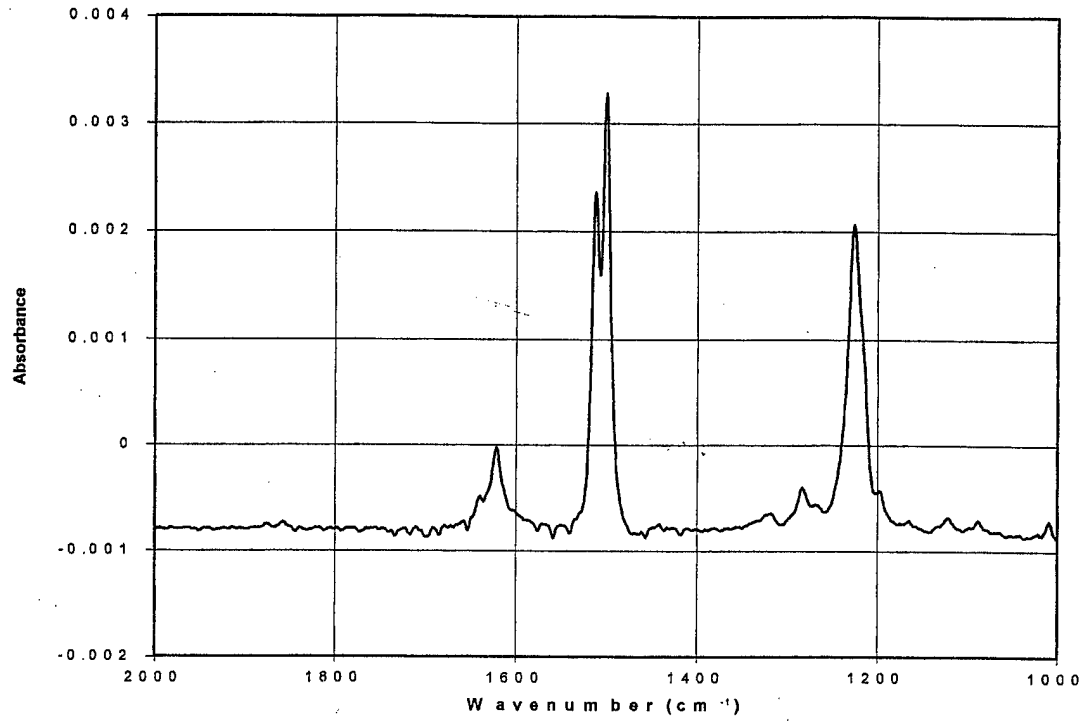

Figure 23. RAIR spectrum of vapor-deposited ODA film on an aluminum substrate. The film thickness was approximately 40 Å.

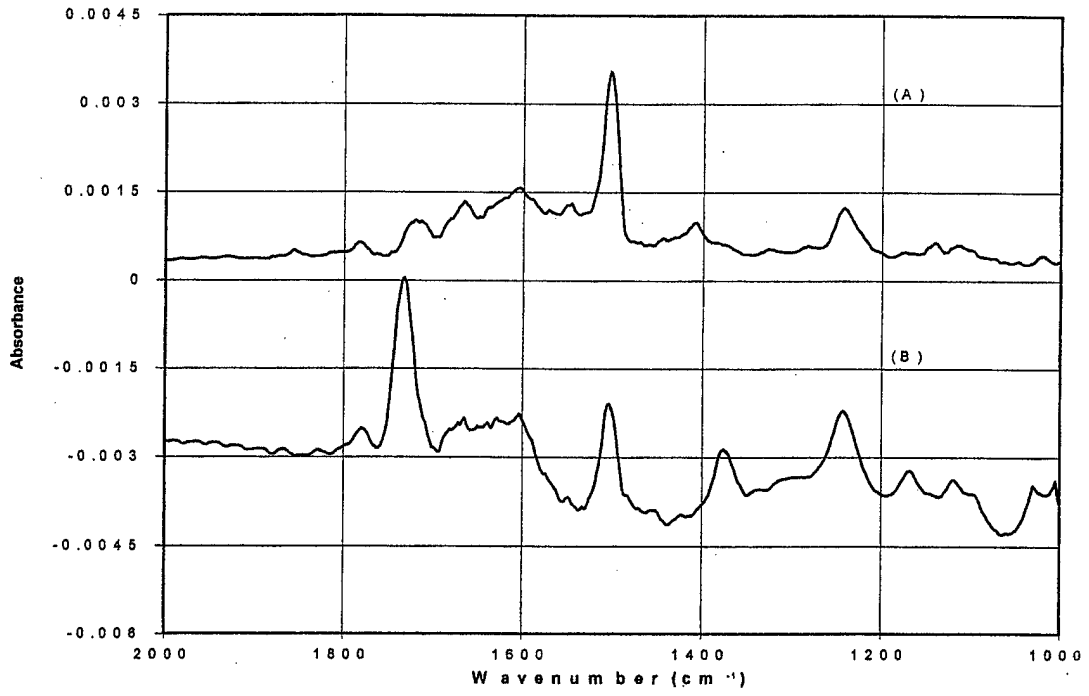

Figure 24. RAIR spectrum of vapor-deposited PMDA/ODA film on an aluminum substrate (A) - as-deposited and (B) - after thermal imidization at 200°C. The film thickness was approximately 30 Å.

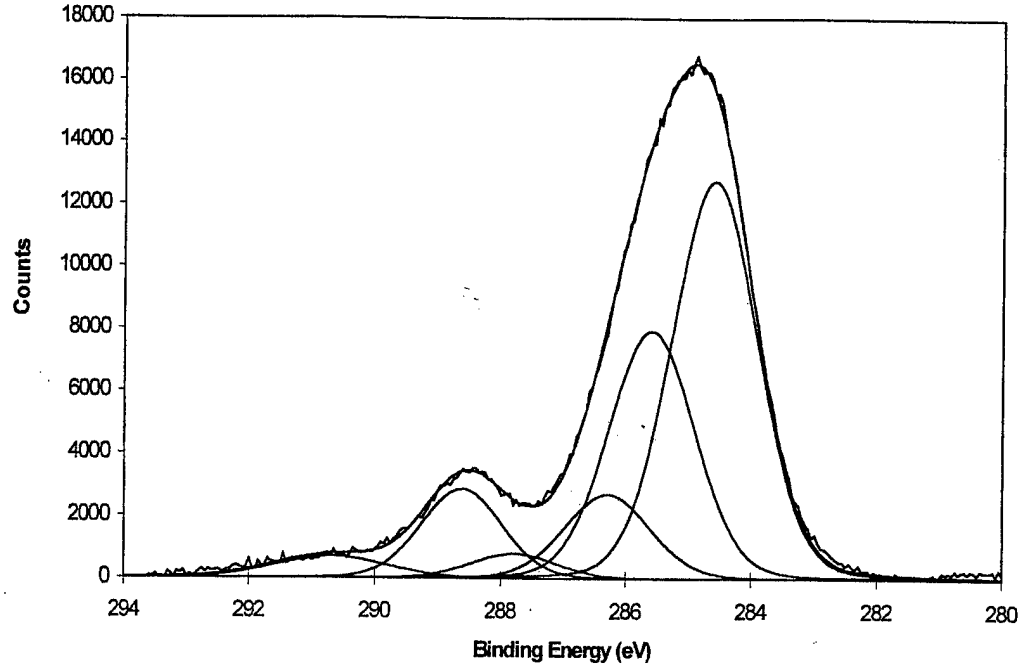

Figure 25. C(1s) XPS spectrum of vapor deposited PMDA/ODA film on aluminum after thermal imidization.

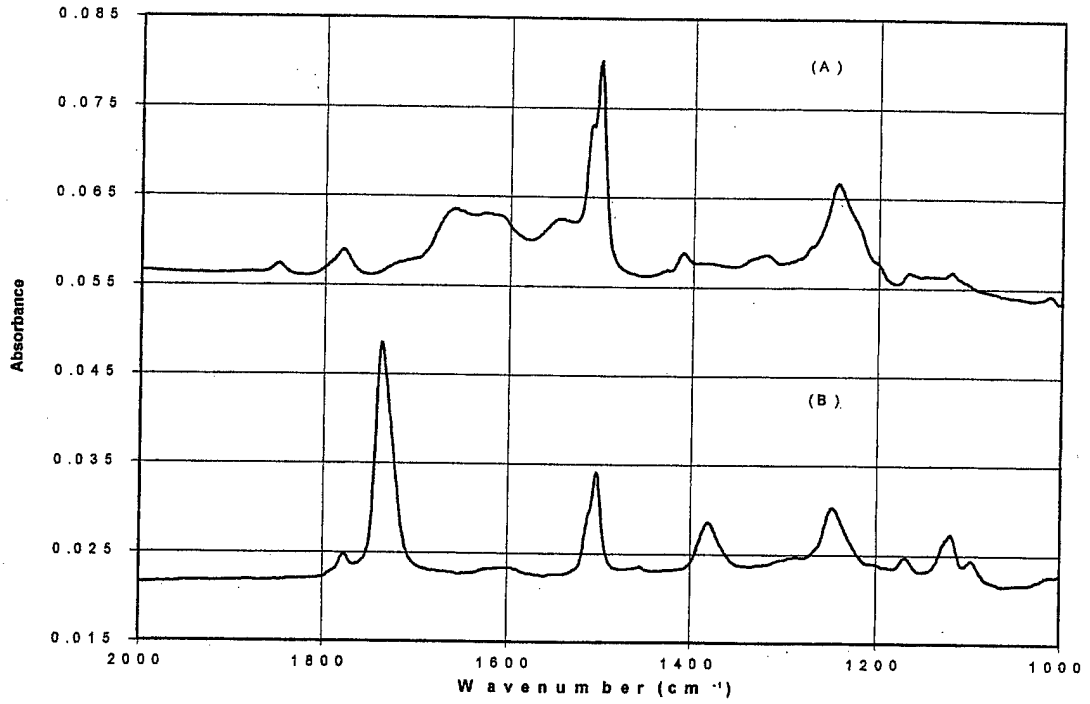

Figure 26. RAIR spectra of thick (ca. 2000 Å) vapor-deposited PMDA/ODA films (A) - as-deposited and (B) - after thermal imidization.

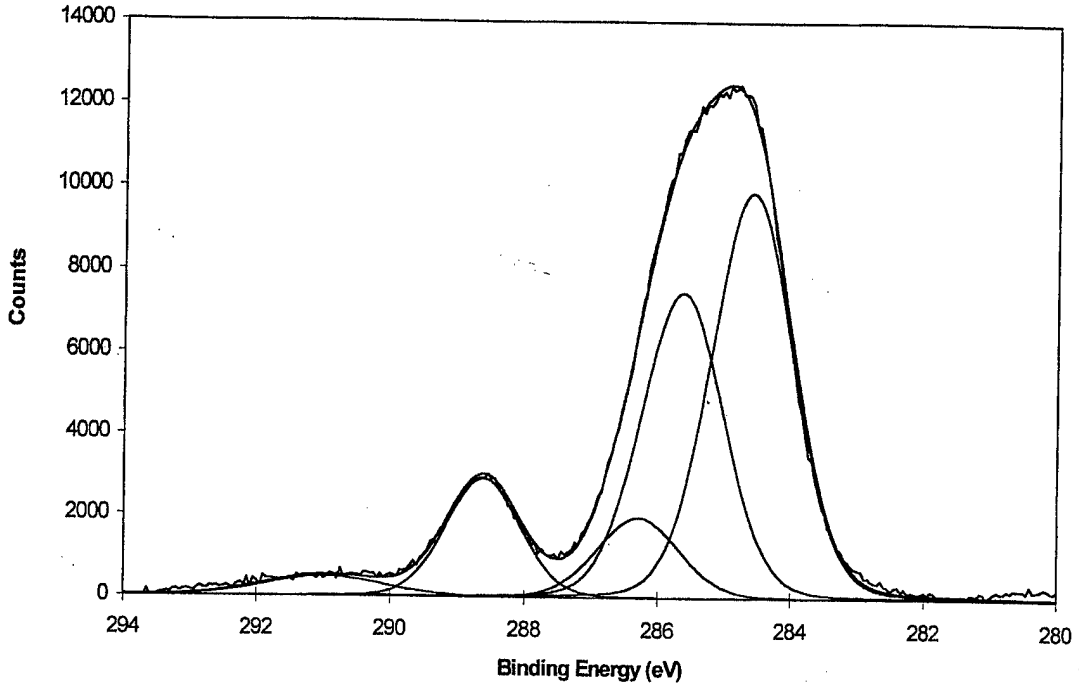

Figure 27. C(1s) XPS spectrum of thick (ca. 2000 Å) vapor-deposited PMDA/ODA film after thermal imidization.

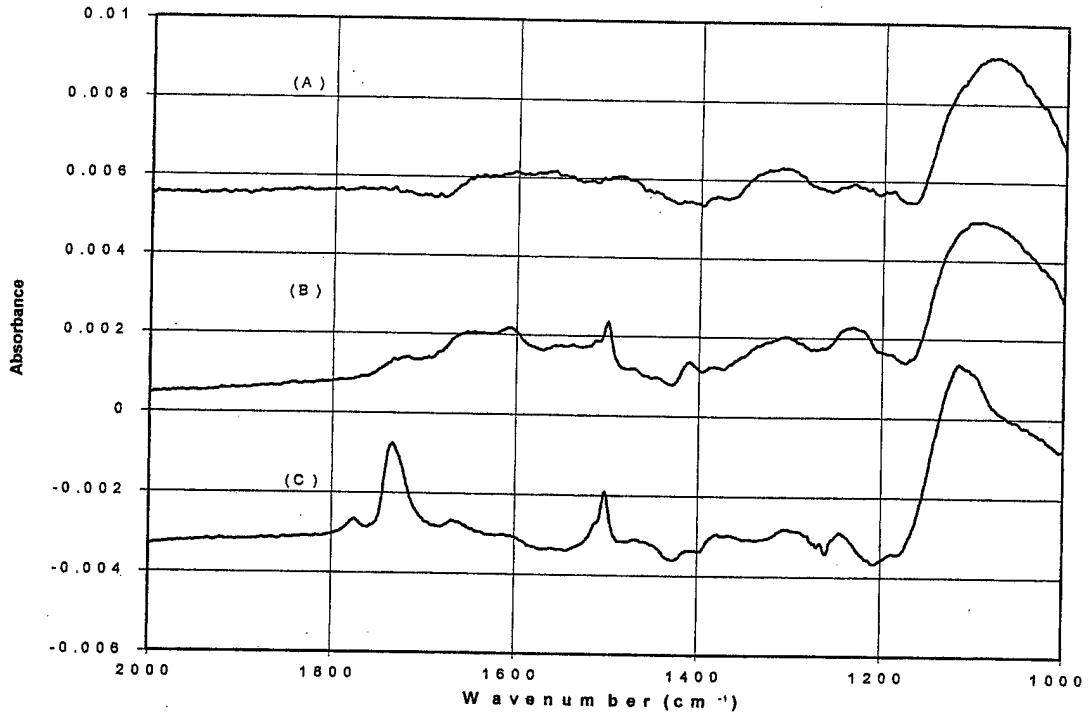

Figure 28. RAIR spectrum of a silanated aluminum surface (A) - as-deposited, (B) - after spin-coating with PMDA/ODA polyamic acid, and (C) - after thermal imidization.

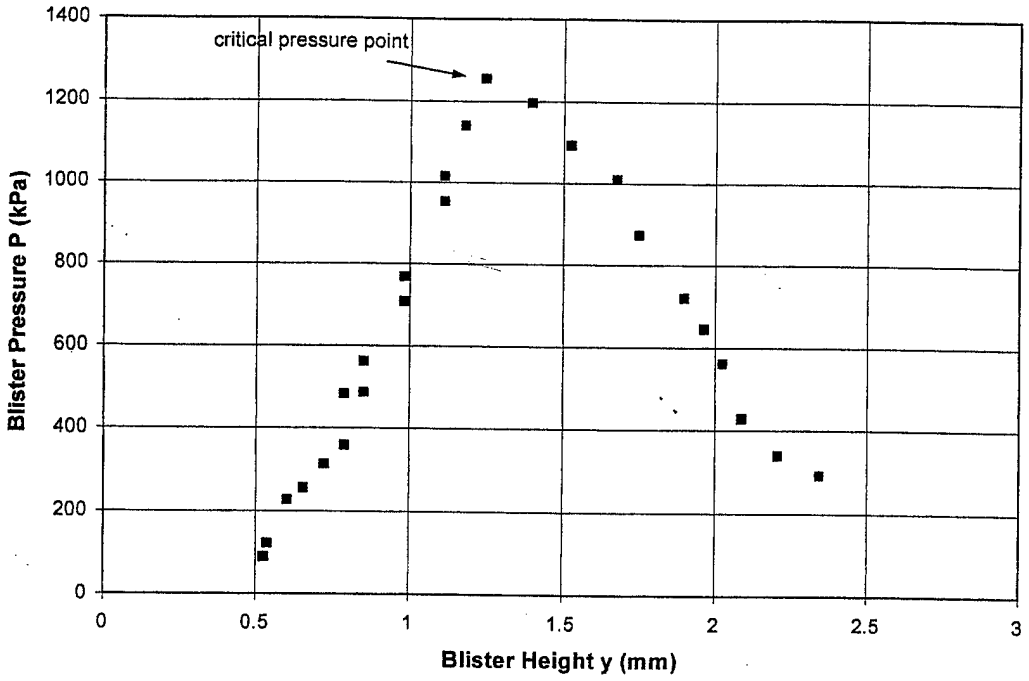

Figure 29. Pressure vs. blister height for PMDA/ODA polyimide film on aluminum.

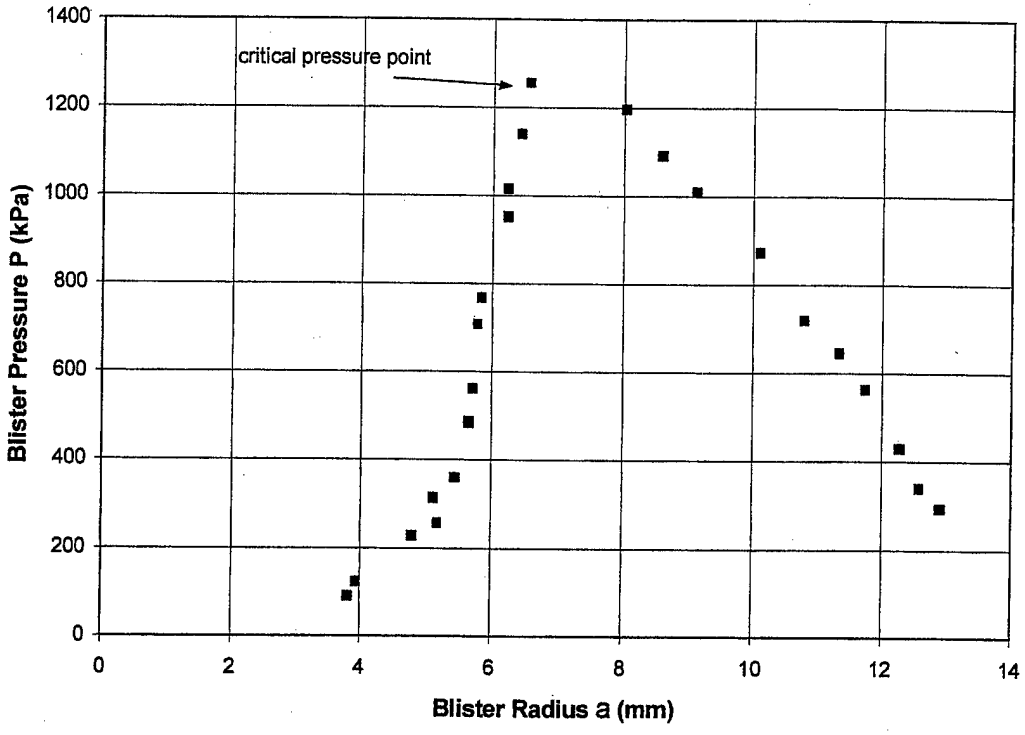

Figure 30. Pressure vs. blister radius for PMDA/ODA polyimide film on aluminum.

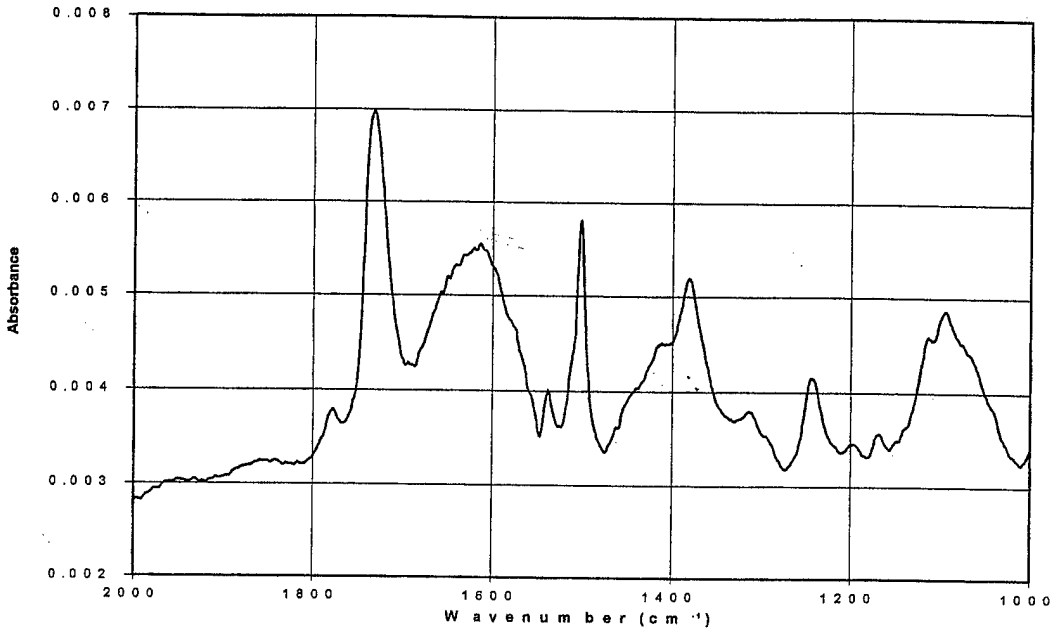

Figure 31. RAIR spectrum of aluminum failure surface after blister test.

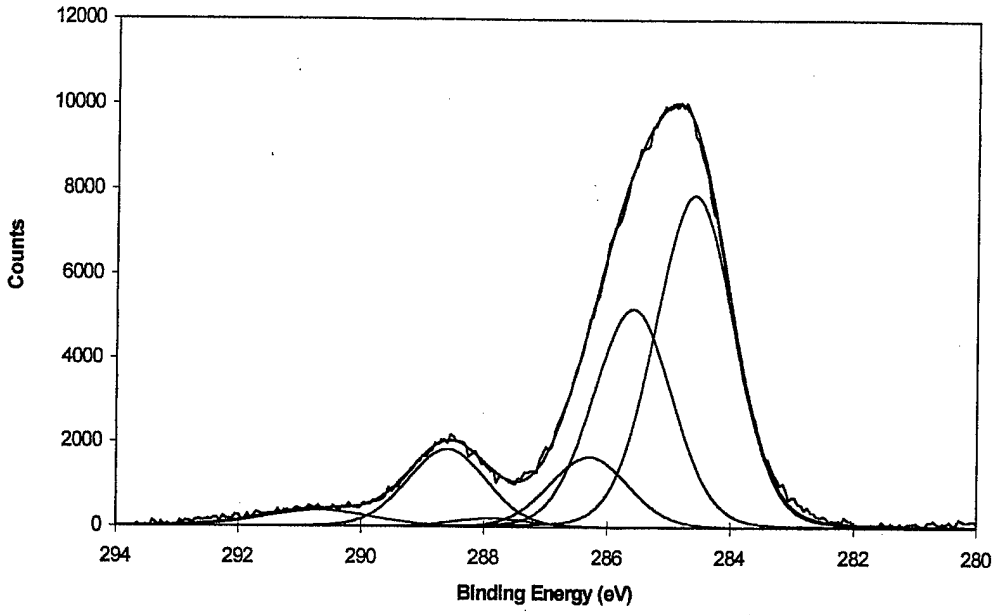

Figure 32. C(1s) XPS spectrum of aluminum failure surface after blister test. The specimen was prepared by vapor-deposition of PMDA/ODA onto an aluminum substrate, thermal imidization of the film, spin-coating of PMDA/ODA polyamic acid from solution in NMP, and thermal imidization of that film.

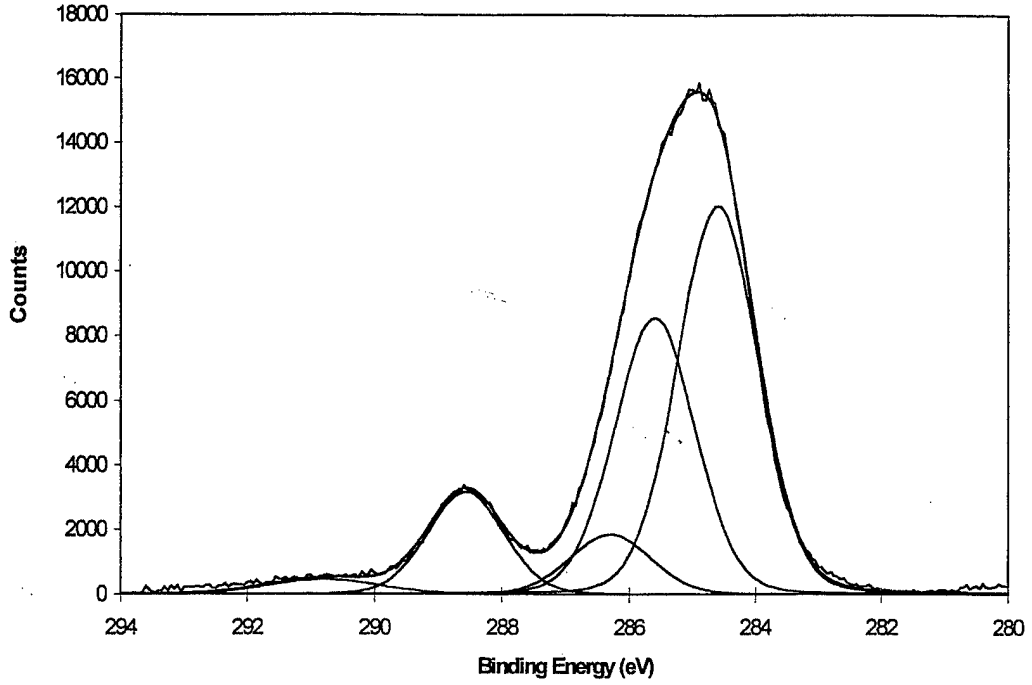

Figure 33. C(1s) XPS spectrum of polyimide failure surface after blister test. The specimen was prepared by vapor-deposition of PMDA/ODA onto an aluminum substrate, thermal imidization of the film, spin-coating of PMDA/ODA polyamic acid from solution in NMP, and thermal imidization of that film.

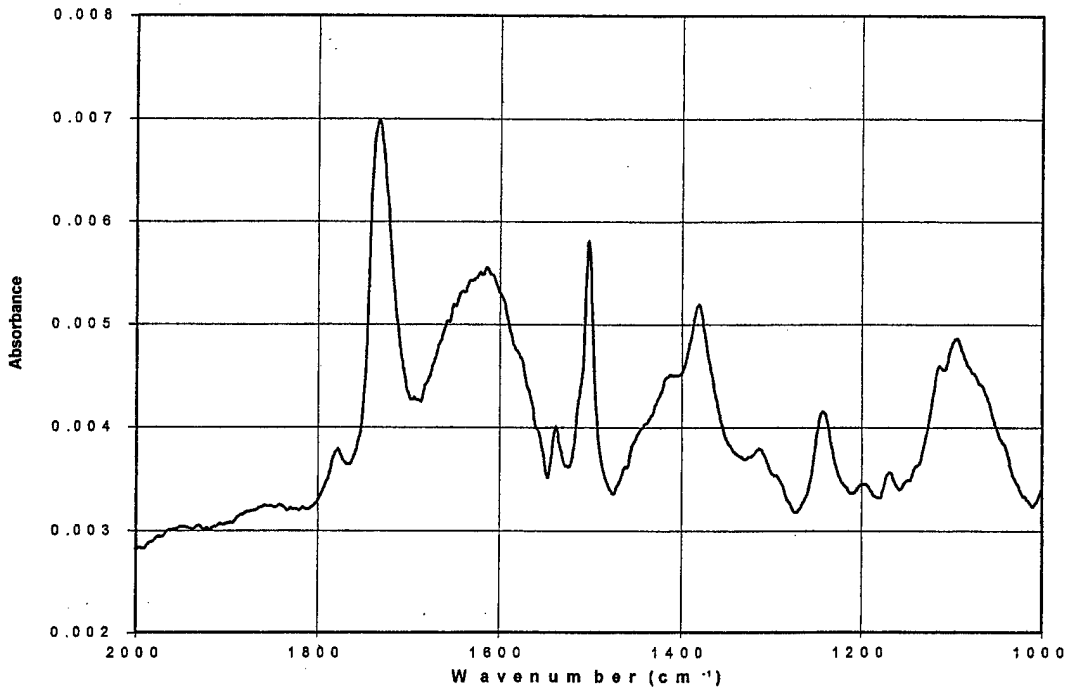

Figure 34. RAIR spectrum of the aluminum failure surface of a specimen prepared by spin-coating PMDA/ODA onto a polished substrate.

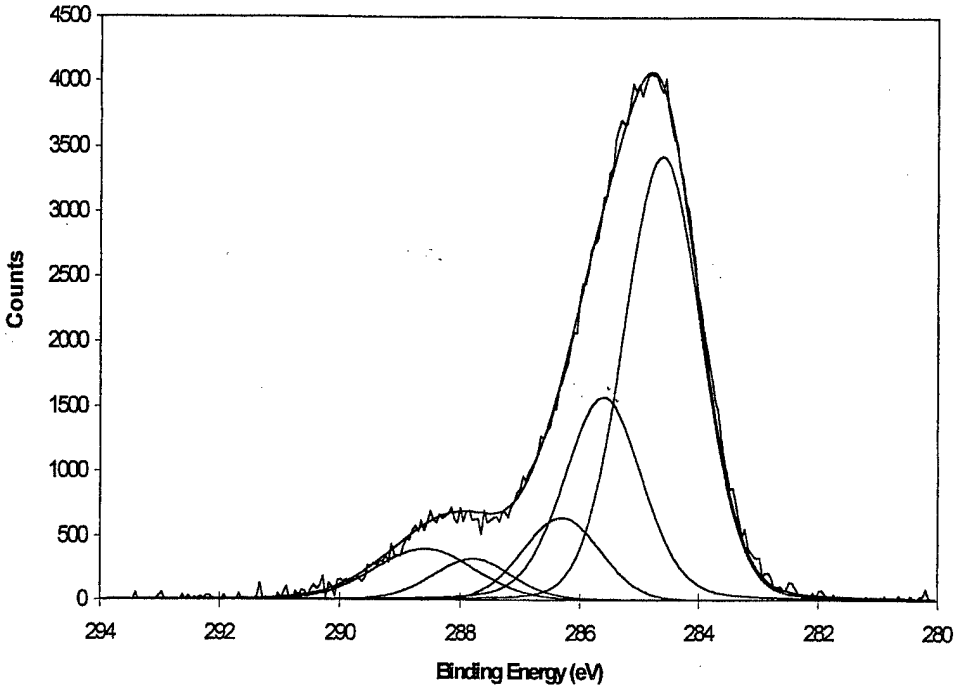

Figure 35. High-resolution XPS C(1s) spectra obtained from the aluminum failure surface of a specimen prepared by spin-coating PMDA/ODA onto a polished substrate.

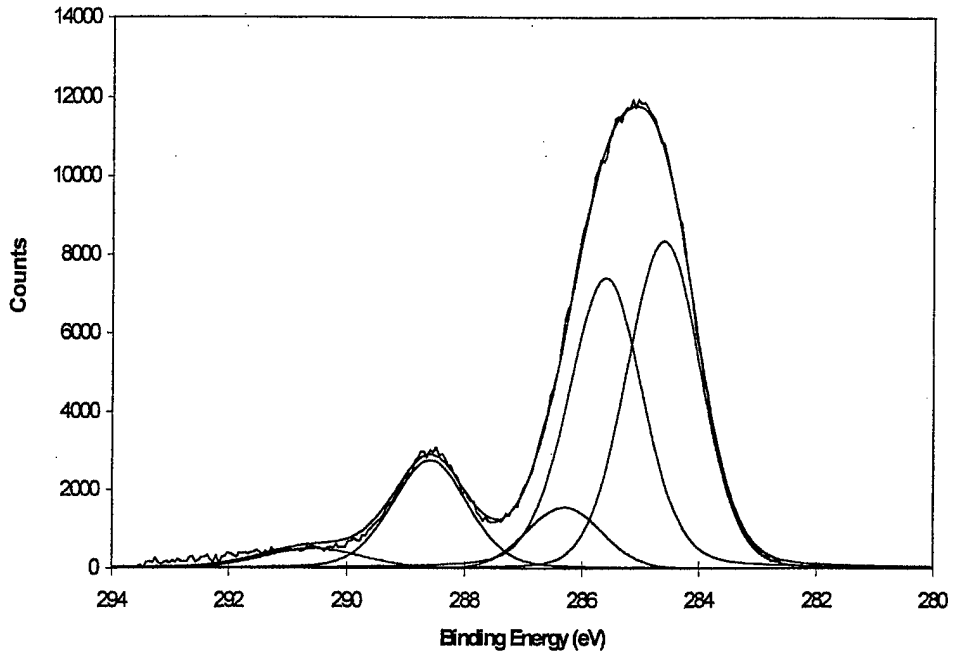

Figure 36. High-resolution XPS C(1s) spectrum obtained from the polyimide failure surface of a specimen prepared by spin-coating PMDA/ODA onto a polished substrate.

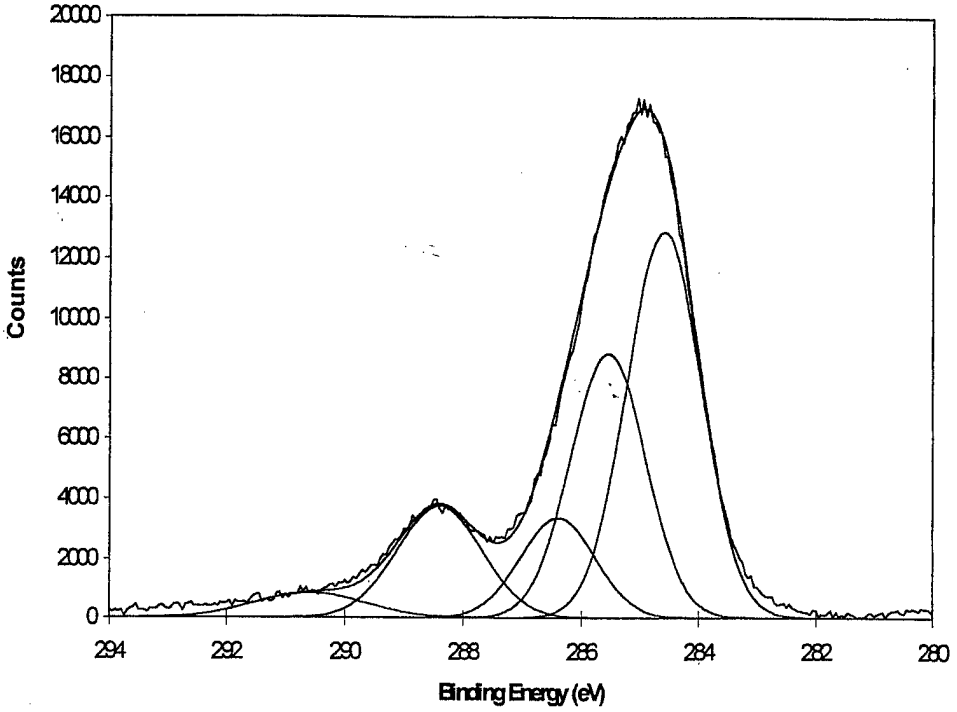

Figure 37. High-resolution C(1s) XPS spectrum obtained from the aluminum failure surface of a blister test specimen prepared by spin-coating PMDA/ODA onto an aluminum substrate that was silanated with γ-APS.

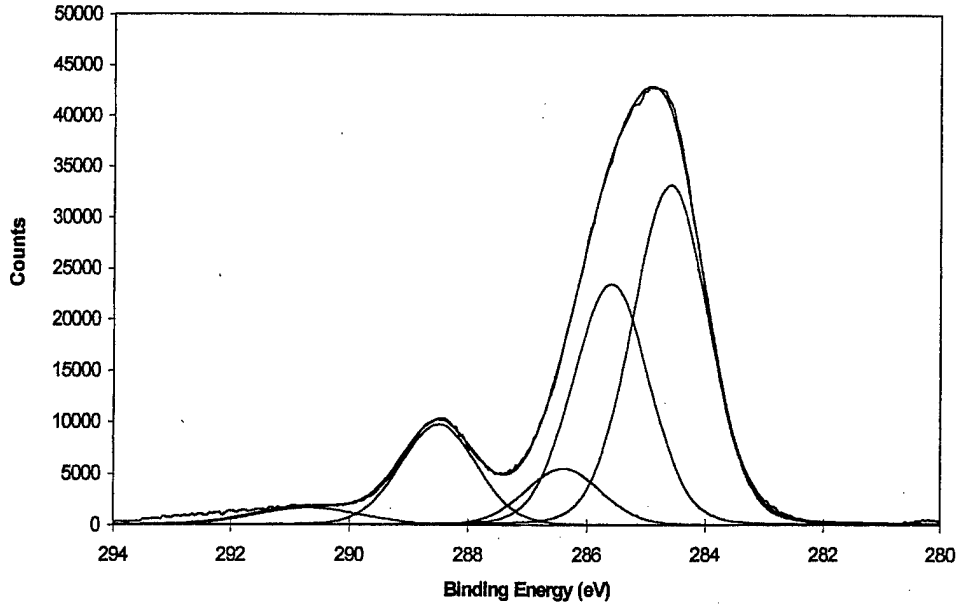

Figure 38. High-resolution XPS C(1s) spectrum obtained from the polymer failure surface of a blister test specimen prepared by spin-coating PMDA/ODA onto an aluminum substrate that was silanated with γ-APS.

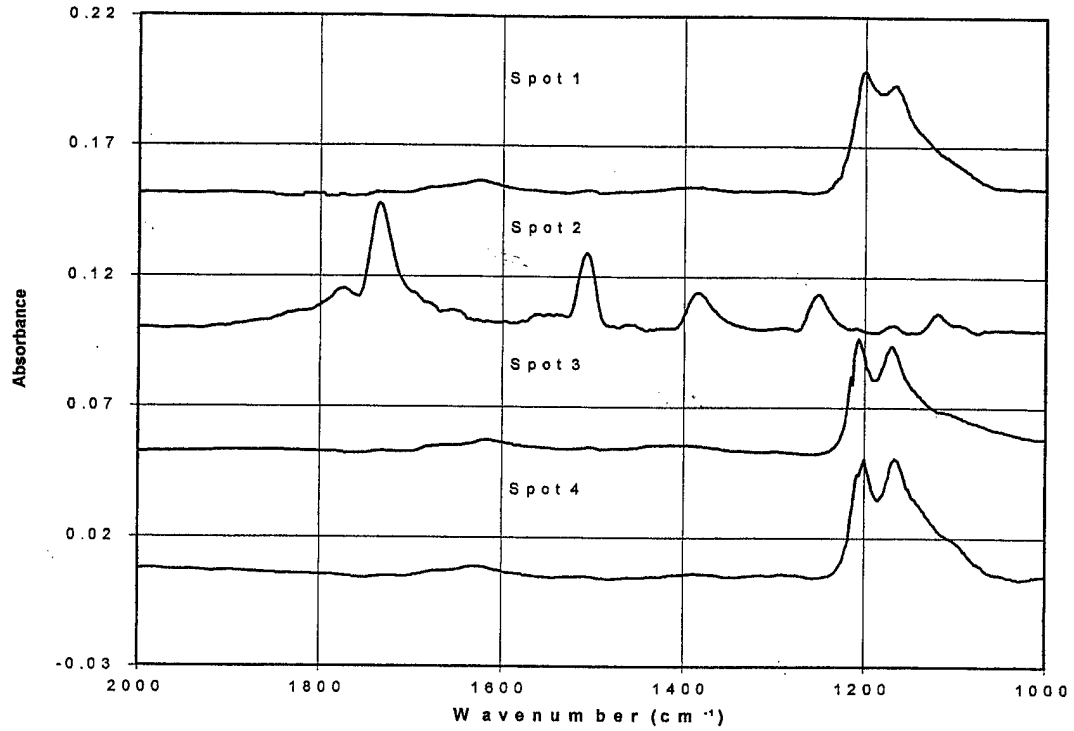

Figure 39. RAIR spectra obtained from several randomly chosen spots on the aluminum failure surface of a blister test specimen prepared by spin-coating PMDA/ODA onto an aluminum substrate that was silanated with γ-APS.

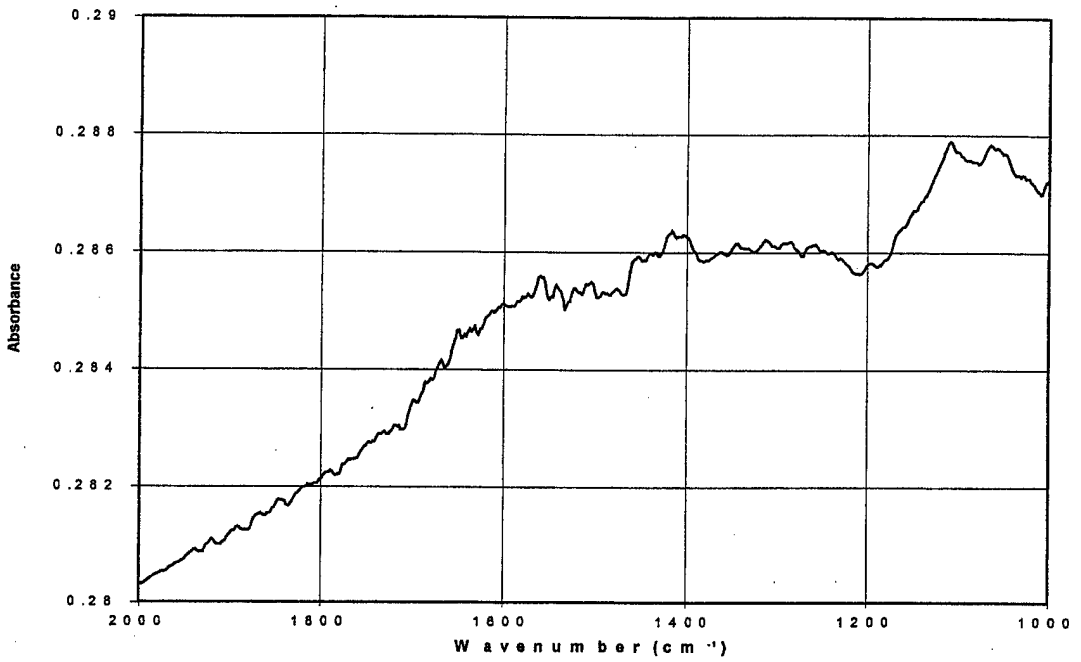

Figure 40. RAIR spectra of gold failure surface of spin-coated PMDA/ODA polyimide film after blister test.

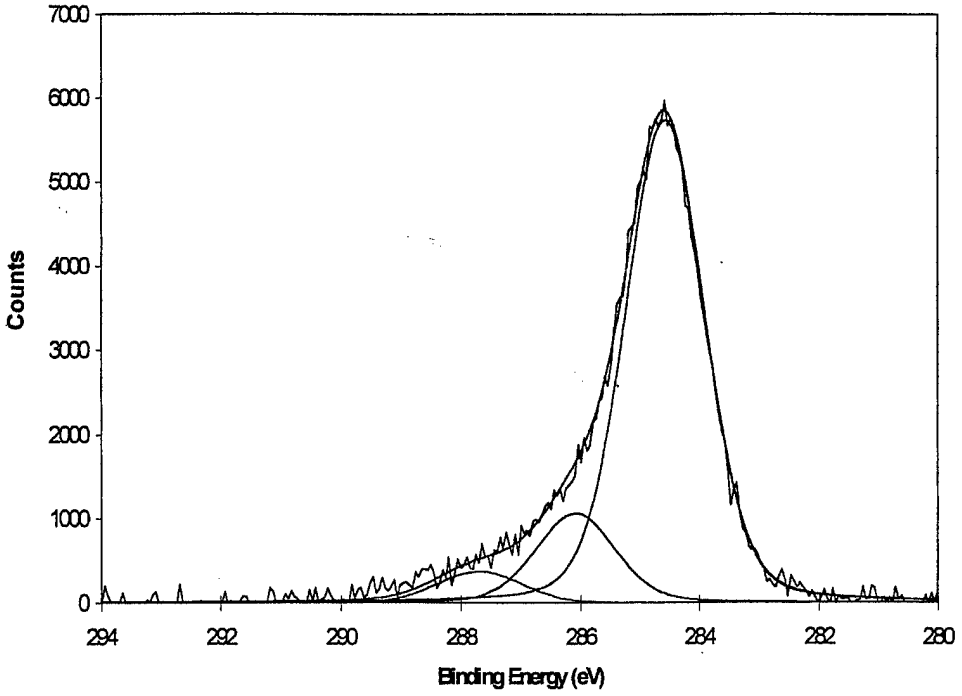

Figure 41. XPS C(1s) spectrum of gold failure surface of spin-coated PMDA/ODA polyimide film after blister test.

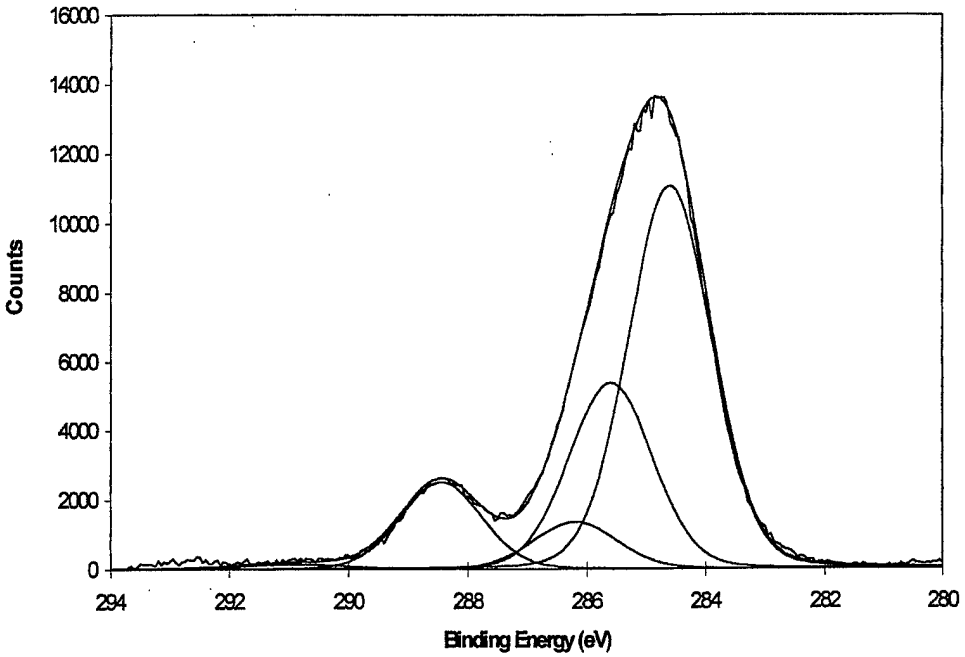

Figure 42. XPS C(1s) spectrum of polymer failure surface of spin-coated PMDA/ODA polyimide film on gold after blister test.

Report Distribution List

Addresses	Number of Copies
Scientific Officer Code: 1131N Peter P. Schmidt Office of Naval Research 800 North Quincy Street Arlington, VA 22217-5000	3
Administrative Grants Officer Office of Naval Research Resident Representative Chicago Regional Office Federal Bldg., Room 208 536 South Clark Street Chicago, IL 60605-1588	1
Director, Naval Research Laboratory Attn: Code 2627, 4555 Overlook Drive Washington, DC 20375-5326	1
Defense Technical Information Center 8725 John J. Kingman Road STE 0944 Ft. Belvoir, VA 22060-6218	2